NUCLEATION AND CRYSTAL GROWTH FROM MELTS

A Thesis submitted for the degree of Ph.D.

in the

University of London

by

Dhayan Kirtisinghe, B.Sc.

Department of Chemical Engineering,

Imperial College of Science and Technology,

London, S.W.7.

July, 1964.

ABSTRACT

Breeding in supercooled melts of benzophenone is ascribed to the presence of microcrystalline particles or dusts on the surface of the innoculating seed crystal. A crystal suitably treated to avoid surface contaminents has been shown to be capable of growth as a single crystal even in highly supercooled melts.

The very large difference in rate between the stirred and unstirred runs shows that heat transfer is still a major factor, despite the relatively very low growth rates of benzophenone and salol. The rate of growth of the (001) benzophenone face increases far more rapidly with bulk supercooling than the rate of heat transfer, and eventually a situation is reached where the growth rate is much larger than could be accounted for by the experimentally measured coefficient of heat transfer.

The use of thermocouples have served to illustrate that one possible explanation for such a result was a mechanism of heat conduction through the crystal due to non-uniformity of surface temperatures. These experiments also show that the rate of growth of the (010) salol face was determined by the surface supercooling and was quite independent of the degree of agitation in the melt.

Measurements in fine glass capillaries at low supercoolings have

shown that the capillary growth rates could be much smaller than the corresponding rate of growth of an unrestricted crystal from the bulk of the melt, and also keep decreasing with time of observation. It follows therefore that the capillary rates do not approximate surface reaction rates as hitherto assumed. The abnormally low rates of growth observed within the capillary may be due to the gradual growing out of surface deformities to the walls and the mechanical introduction of surface defects on such a crystal is seen to reactivate the growth processes.

ACKNOWLEDGEMENTS

I would like to thank Dr. R. F. Strickland-Constable for helpful supervision and valuable advice given throughout this course of study. I am also indebted to several of my colleagues for useful discussions.

Grateful acknowledgement is made to the British Council for financial assistance and to the Tea Research Institute of Ceylon for leave of absence.

CONTENTS

CHAPTER 1

THEORY OF NUCLEATION AND GROWTH

1.1 General Introduction

Although much theoretical work on the kinetics of crystal growth has been carried out and reported in the literature, accurate measurements on the kinetics of growth from the liquid phase are largely confined to a number of measurements in capillary tubes. A principal difficulty is one common to all interphase work, namely the uncertainties introduced by concentration and temperature gradients at the interface.

In the present work growth from the melt of various crystals has been studied. In the first instance extremely slow growing crystals were chosen with a view to eliminating, as far as possible, the temperature gradients in the melt: this elimination was only partly successful even with high stirring rates. Other methods of measuring the true surface kinetics were however tried with more success: this work has led onto other types of experiments in which rates of growth of free growing crystals were compared with rates of growth in capillaries: rather unexpected results were obtained which it is believed should throw considerable light on the older measurements in capillary tubes, and on the theories of crystal growth in general.

1.2 Nucleation

Before starting work on growth-rates some experiments were carried out on a particular aspect of nucleation from the melt. For this reason a brief account of the current theories on nucleation will be given.

The thermodynamic potential of the solid has to be lower than that of the melt before nucleation or growth can occur, i.e. a state of supercooling must first be achieved. Nucleation may then occur spontaneously in the bulk of the fluid phase (homogeneous nucleation), or may occur on the walls of the vessel or on dust particles in suspension (heterogeneous nucleation). The latter is the more commonly encountered form of nucleation on account of the almost universal occurrence of dusts and other foreign contaminents.

Volmer[1], Becker and Doring[2] and others found it possible to derive from kinetic theory a solution for the rate of homogeneous nucleation, which involved a thermodynamic analysis of the various free energies involved. The work of nucleus formation (W) is the sum of the free energy of formation of the surface and that of the bulk of the particle, and for a spherical particle of radius r,

$$W = \frac{4}{3} \pi \sigma r^2 \qquad \text{.....(1)}$$

where σ is the surface tension.

The Gibbs-Thomson equation gives,

$$r = \frac{2 M \sigma}{RT \rho \ln \frac{P}{P_{sat}}} \qquad \ldots\ldots (2)$$

Where P and P_{sat} are the vapour pressures over a liquid droplet of radius r and the saturation vapour pressure, M the molecular weight and ρ the density of the droplet. T is the absolute temperature and R the gas constant.

Analysis of the kinetics of the process then lead to the well known result for the nucleation rate in an Arrhenius type equation of the form,

$$I = B \exp. \left[- \frac{16 \pi \sigma^3 M^2}{3 R^3 T^3 \rho^2 (\ln \frac{P}{P_{sat}})^2} \right] \qquad \ldots\ldots (3)$$

The pre-exponential frequency factor B is relatively insensitive to small changes of temperature, and is sometimes treated as a constant.

Tamman[3] observed the rates of nucleation in a number of supercooled organic melts and his results were found to be in good agreement with the form equation 3, at low supercoolings. The subsequent fall in the nucleation rate observed experimentally at still lower temperatures, or higher supercoolings being ascribed

to viscous factors, not included in the above treatment, becoming rate controlling.

In the present study, homogeneous nucleation is of interest only in so far as it had to be carefully avoided, and studies were made in that part of the metastable region where the probability of such an event was extremely low, and other precautions such as heat treatment of the melt above the melting point and filtration were employed to minimise the risk of what might seemingly be, autonucleation.

Foreign particles, or surfaces are also known to have a catalysing influence on nucleation, by requiring a smaller free energy of formation of a critical nucleus, than is normally required for homogeneous nucleation. Mechanical shock, attrition and radiation of several forms are also methods known to induce heterogeneous nucleation in melts. In addition nuclei can be produced by what has been termed the 'breeding' process, that is to say nuclei are produced by the presence in the solution or melt of crystals of the same substance. Little reference to this phenomenon is found in the literature. Mason[4] in a study of the mechanism of breeding in supersaturated aqueous solutions of magnesium sulphate heptahydrate concluded that microcrystalline particles on the surface of the seed, the breaking off of needle-like growths, crystal splintering

and attrition were the factors involved in breeding in this instance.

In view of the little understood nature of this process, a short study was made of 'breeding' by innoculation of supercooled melts with a seed crystal of the same substance. This study preceded the main work on crystal growth.

1.3 Crystal growth

Once nucleation has been achieved, resistance to growth is due partly to a transport process in the fluid phase (which in the case of a melt is the transfer of heat), and partly to the resistance of the surface reaction.

The mechanism of the surface reaction will be discussed in the immediately following paragraphs: and the relation between the surface reaction and the transport process will be taken up in section 1.4.

a) Collision theory mechanism:- The kinetics of the condensation of a vapour onto a liquid surface has been worked out by the collision theory for a condensing vapour on the basis that the net rate of growth of the liquid from the vapour is the difference between the opposite and independent processes of condensation and evaporation.

By the kinetic theory, at the saturation pressure (P_{sat})

$$R_c = R_e = (2 \pi m k T)^{-\frac{1}{2}} P_{sat} \quad \ldots\ldots (4)$$

Where R_c and R_e are the rates of condensation and evaporation respectively, k is the Boltzmann constant and m is the mass of a molecule.

At an external pressure P, such that $P > P_{sat}$, while the evaporation rate remains unchanged

$$P_c = (2 \pi m k T)^{-\frac{1}{2}} P \quad \ldots\ldots (5)$$

Therefore the net rate of condensation R_n

$$R_n = R_c - R_e = (2 \pi m k T)^{-\frac{1}{2}} (P - P_{sat}) = (2 \pi m k T)^{-\frac{1}{2}} \Delta P \quad \ldots\ldots (6)$$

ΔP being the difference between the external pressure P and the saturation vapour pressure P_{sat}.

If only a fraction α of all the colliding molecules actually condense into the lattice the remainder being reflected, then,

$$R_n = \alpha (2 \pi m k T)^{-\frac{1}{2}} \Delta P \quad \ldots\ldots (7)$$

For a crystal growing from the melt, a similar mechanism is sometimes assumed. The net rate of growth is considered to be the difference between the gross rates of solidification and melting.

Their exact magnitudes are uncertain, but since each of these rates are continuous functions of temperature, it follows that the net rate of growth for small supercoolings is proportional to ΔT, i.e. $R_n = C.\Delta T$.

b) Two dimensional nucleation theory of growth:- This theory was originally developed by Volmer[5] who postulated a mechanism whereby molecules were first absorbed on the surface of the crystal and subsequently attach themselves in positions which were most favourable, viz. at the edge of an incomplete layer on the crystal surface. This process occurs until all such layers are complete leaving a flat surface on a molecular scale. After completion of one layer, growth may continue only after the formation of a new monolayer nucleus, by a process termed two dimensional nucleation. The rate governing step of this process being the formation of a nucleus, completion of a layer once formed being relatively quick.

The size of this critical island nucleus for a condensing vapour has been expressed by the Gibbs equation

$$r = \frac{C_i}{\ln\left(1 + \frac{\Delta P}{P_{sat}}\right)} \qquad \ldots\ldots\ldots\ldots\ldots\ldots\ldots\ldots\ldots\ldots\ldots\ldots (8)$$

where C_i is a constant for a particular face.

As $\Delta P \rightarrow 0$, r increases very rapidly, decreasing the probability

of its formation. Burton, Cabrera and Frank[6], assuming values for the edge free energies of these nuclei, were able to apply the two dimensional nucleation theory to the approximate calculation of growth rates: it appeared that about 50% supersaturation would be required for a reasonable probability of formation of such a nucleus. The rate of formation would be negligible around the 1% level of supersaturation, in spite of the fact that growth rates are usually easily measurable at this supersaturation.

c) Frank's screw dislocation theory:. Frank[7] introduced the concept that screw dislocations could possibly account for the above mentioned very large difference in rate between surface nucleation theory and practice. A screw dislocation would give rise to a self-perpetuating spiral growth step, which would eliminate the need for the formation of a two-dimensional nucleus, and which would therefore be capable of accounting for the large rates observed experimentally.

The existance of spiral growth steps in the mechanism of growth has been clearly demonstrated, for certain cases. For instance, Albon and Dunning[8] in a study of the growth behaviour of selected areas of a sucrose crystal, found that growth was imperceptible at low supersaturations in the absence of a dislocation with a screw

component and Sears[9] finds evidence for a screw dislocation mechanism of growth in certain faces of a lead iodide crystal growing from the melt.

d) Layer by layer growth:- Bunn and Emmett[10] have observed in the case of aqueous solutions of inorganic electrolytes, that growth appears to depend on the spreading of a sequence of layers from a particular point on the crystal surface. This mechanism appears to be basically different from the spiral growth mechanism, although it has been claimed that the growth of the layers may originate in a pair of opposite handed screw dislocations.

e) Structure sensitivity of growth rates:- The growth rates of some substances have been found to vary considerably at low supersaturations. This variation in rate has been attributed to structural defects. Thus, Hillig[11] studying the effect of crystal perfection on growth kinetics of ice crystals, observed that imperfect crystals have a very much higher growth rate than perfect crystals: viz. 300 times higher for imperfect crystals at 0.03 deg C supercooling than for perfect ones, and that damage to a crystal could also enhance its growth rate.

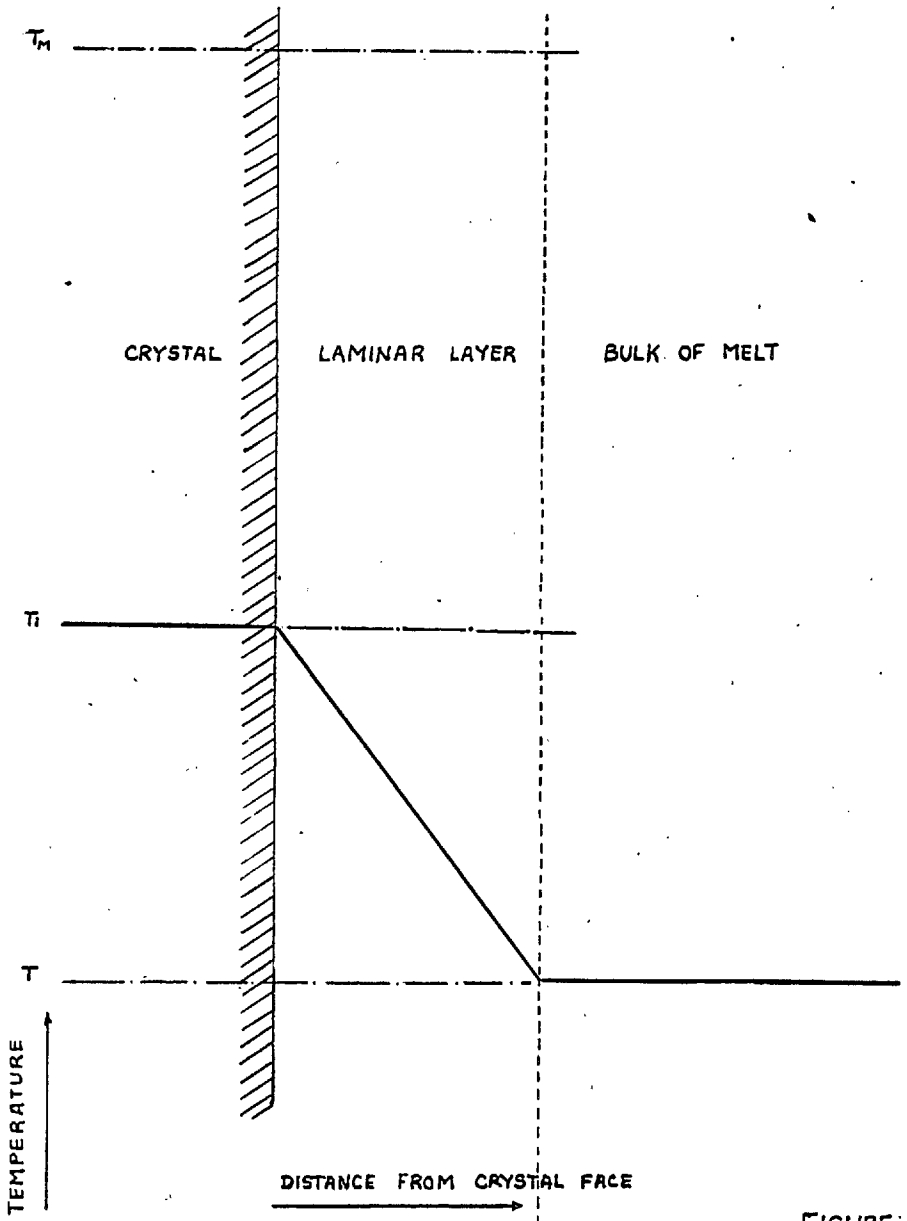

FIGURE 1.

TEMPERATURE PROFILE ACROSS THE FACE OF A GROWING CRYSTAL.

1.4 Relation between surface reaction and heat transfer processes

The liberation of the latent heat of fusion at the interface of the growing crystal results in an increase of the interfacial temperature (T_i) over that in the bulk of the melt (T), with a resulting reduction in growth rate. Therefore an understanding of the kinetics of the surface reaction demands a knowledge of this surface temperature.

Referring to figure 1, in general the surface reaction rate, R_n, may be expressed in the form;

$$R_n = f(T_i - T_m) \quad \ldots\ldots (9)$$

where T_m is the melting point of the material and f is an unspecified function.

The rate of heat transfer, Q, can be expressed by

$$Q = h(T - T_i) \quad \ldots\ldots (10)$$

where h is the heat transfer coefficient normally assumed to be independent of $(T - T_i)$.

In terms of growth rate (10) may be written

$$R_n = \frac{h}{\rho \lambda} (T - T_i) \quad \ldots\ldots (11)$$

so that the whole process is governed by the pair of equations

$$R_n = f\ (T_i - T_m)$$

and $$R_n = \frac{h}{\rho \lambda} (T - T_i).$$

In principle if h and f ( ) are known, T_i may be eliminated between equations (9) and (11) and the temperature dependence of growth rate determined. The coefficient of heat transfer could in principle be determined by independent measurements.

As already explained, under many conditions T_i will be intermediate between T and T_m. Two extreme cases can also be envisaged: if heat transfer is rapid and surface reaction slow then $T_i \rightarrow T$, and the rate of growth approaches

$$R_n \longrightarrow f\ (T - T_m)$$

the system is 'surface rate controlled'.

If heat transfer is slow and surface reaction rapid then $T_i \rightarrow T_m$ and growth rate will be given by

$$R_n \longrightarrow \frac{h}{\rho \lambda}\ (T - T_m)$$

the system being then said to be under 'heat transfer control'.

Increase in stirring rate will of course increase the rate of

heat transfer, so that T_i tends to increase and to approach T_m: under these circumstances a limiting reaction rate will sometimes be observed at high rates of stirring. Thus Butler[12] observed an initial increase of growth rate of sodium thiosulphate crystals with agitation, but beyond 20 r.p.m. no further increase of growth rate was observed. This is one of the only examples quoted in the literature where the resistance due to a transport process has been shown to have been reduced by agitation to a degree when it ceases to be of importance in determining overall rates: in this case the controlling process is one of mass transfer rather than of heat transfer.

Chapter 2

NUCLEATION

2.1 Introduction

It has been suggested by a few workers in the past that the introduction of a seed crystal to a supercooled melt or a supersaturated solution could not only result in the growth of the parent crystal but under certain circumstances lead to the formation of a new crystal nucleus. This form of heterogeneous nucleation which has been termed "breeding" by Mason and Strickland-Constable,[13] differs from other forms of nucleation in that it requires the presence of a crystal. Among the rare references to this phenomenon can be cited the following:-

Miers[14] was one of the earliest workers to refer to this form of heterogeneous nucleation, which McCabe[15] claims to be among the most important methods in industrial practice. Ting and McCabe[16] made a short study of one aspect of breeding in well stirred supersaturated solutions of $MgSO_4.7H_2O$ and the mechanism by which this process occurs has been studied in much greater detail by Mason.[4] Van Hook[17] also concluded that breeding in well stirred supersaturated solutions of sucrose could be due to the detachment of irregular growths.

No experiments on breeding from melts have ever been described. Experiments on breeding from benzophenone melts were therefore

undertaken, and are described below.

2.2 Apparatus

Experiments were conducted in a constant temperature bath which consisted of a glass tank 9" x 7" and 10" deep with distilled water to a depth of 15". Heat was supplied through an immersion heater regulated by a Sunvic control which in turn was actuated by a mercury-toluene switch fitted with a Sunvic proportioning head. The heat supply could be varied continuously from about 50 watts to a maximum of 1 kilowatt, by introducing a rheostat in series with the heater. A double-bladed propellor, 3" in diameter rotating at approximately 600 r.p.m. provided the agitation required to ensure uniformity of temperature throughout the bath. With this arrangement the final overall control was found to be better than $\pm$ 0.01°C, under the experimental conditions. A second tank to a similar specification was brought into use for the production of seed crystals with treated surfaces.

2.3 Materials and purification

The material used for this investigation was diphenyl ketone (benzophenone), and phenyl salicylate (salol) was also used in the subsequent study of growth. A great deal of research has already

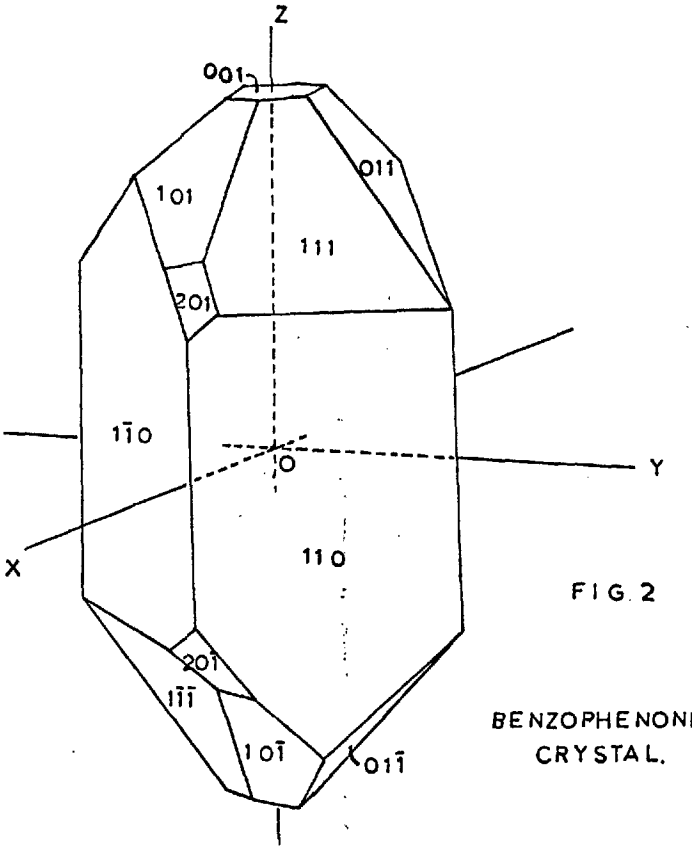

FIG. 2

BENZOPHENONE CRYSTAL.

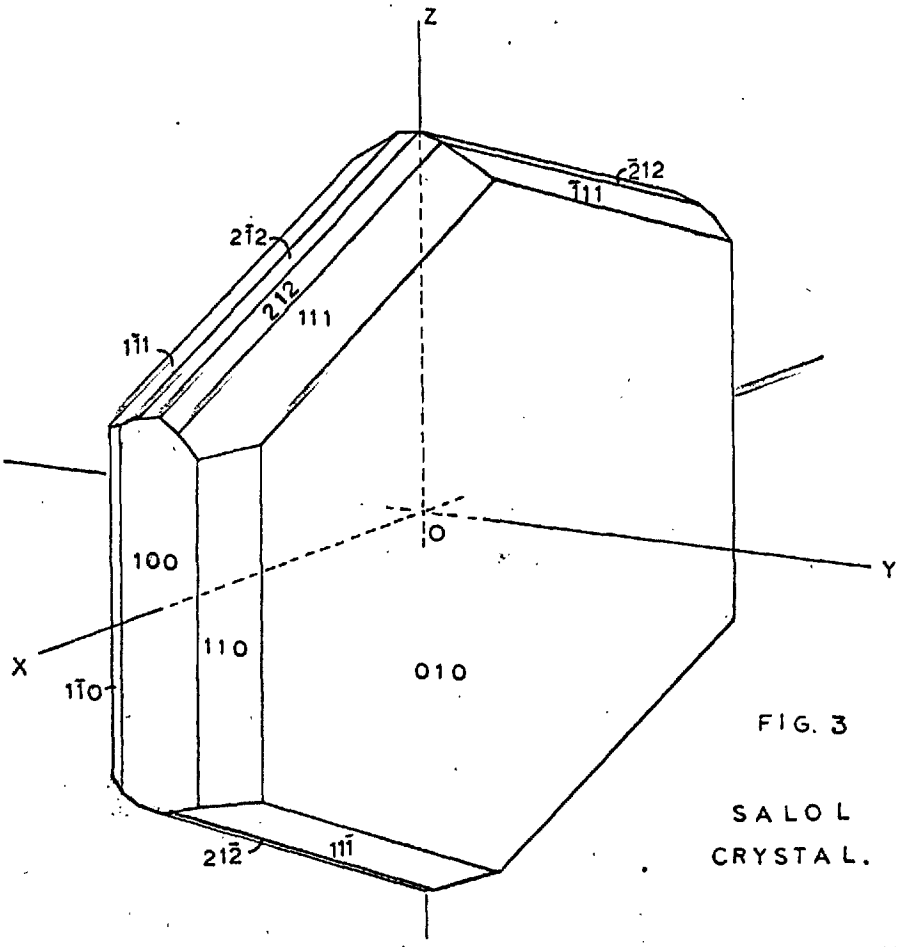

FIG. 3

SALOL CRYSTAL.

been done on these materials; the main advantages they have to offer apart from their relative inertness being ready purification, low melting points, measurable growth-rates over a wide range of supercoolings and the ability to stand large supercoolings for long periods without the complications arising from the event of homogeneous nucleation.

Benzophenone, supplied as a General Purpose Reagent by Hopkin and Williams was purified by double distillation under reduced pressure. The materials so purified melted to a clear transparent liquid at 48.0°C.

2.4 Morphology of benzophenone and salol

Figure 2 is a diagram of an ideal crystal of benzophenone whose morphology has been described by Groth.[18] The crystal belongs to the orthorhombic sphenoidal class and is characterised by three mutually perpendicular diad axes of symmetry. It has four prominent prism faces (110) , but for the most part this investigation has been centred on the small, fast growing, (021) face.

Groth[19] has also described the morphology of salol, which belongs to the orthorhombic holohedral class, with three diad axes

Photograph 1
20 Seconds after immersion

Photograph 2
45 Seconds after immersion.

Photographs 1 and 2 are of untreated seeds mounted on the (001) face.

T_i = 26·2°C ΔT = 21·8°C

X 1·5

Photograph 3
6 Seconds after immersion

Photograph 4.
12 Seconds after immersion

Photographs 3 and 4 are of untreated seeds mounted on the (010) face.

T_i = 26·2°C ΔT = 21·8°C

X 1·5

Photograph 5
6 Seconds after immersion

Photograph 6.
30 Seconds after immersion.

Photographs 5 and 6 are of seeds with treated surfaces mounted on the (001) face.

T_i = 26·5°C ΔT = 21·5°C

X 1·5

mutually at right angles. Figure 3 is a diagram of an idealised crystal of salol, which is a thin tabular crystal with two prominent and equivalent (010) faces. The behaviour of these faces have been studied under a variety of conditions.

2.5 Seed crystals

Seed crystals of benzophenone for use in both nucleation and growth studies were prepared by solidifying a smear of benzophenone melt on a glass rod followed by development of these crystals to a length of 3 - 5 mm. by immersion in its supercooled melt at 36°C. These crystals were detached from the glass rod and stored for subsequent use as and when required.

Benzophenone crystals were mounted for use by touching the (001) crystal face (Figure 2) with a warm glass spike. The slow growing (110) were found to be unsuitable for mounting, as these faces exhibit a marked increase in the tendency to produce more crystals from the point of attachment, with an orientation different to that of the seed on re-immersion in the supercooled melt. (Compare photographs 2 and 4.)

2.6 Inoculation of supercooled benzophenone melts with 'untreated' seed crystals

25 ml. samples of the purified benzophenone melt, contained in sample tubes of 3 cm. O.D. were first superheated by warming in a water bath for approximately 5 minutes, prior to cooling down to the experimental conditions. Once temperature equilibrium was attained the crystal was mounted as described in section 2.5 and lowered on its supporting glass rod to a position just below the surface of the melt. It was then held in this position by clamping the glass rod and subsequently withdrawn for examination under a polarising microscope.

The crystal continued to grow on its mount as a single crystal when lowered into a melt whose supercooling was less than 3.5°C, and showed little tendency to nucleate elsewhere in the melt. When on occasion it did the new nuclei formed were invariably found floating on the surface of the melt, completely detached from the seed. The numbers of such crystals were small, seldom in excess of two.

Examination under a polarising microscope revealed that the new growth on the seed crystal had the same optical properties as the parent material and that the interface between the original

seed and the new crystal material was free of growths with a crystallographic orientation different to that of the seed.

At slightly higher supercoolings (ΔT's of 7-9°C) the seeds still continued to grow as a single crystal, but with an increase of the tendency to produce fresh nuclei at the surface of the melt.

Microscopic examination of the interface between the parent seed and the new layers of growth deposited under conditions of 7 - 9°C bulk supercooling, employing transmitted polarised light revealed some small areas which had a different extinction angle and therefore a different crystallographic orientation to that of the parent material. These areas were eventually covered over with material of the same optical nature and crystallographic orientation as that of the seed, suggestive of some form of 'surface healing'.

At supercoolings in excess of 11°C, i.e. below 37°C, needle-like growths appeared (see Photographs 1 - 4) seemingly from the surface of the seed crystal. These needles developed in size for upto 2 - 3 minutes and then detached themselves from the parent crystal, probably on account of their weight. Photograph 4 show two newly formed crystals which have detached themselves from the parent crystal falling away. Very soon after this photograph was

taken the tube became opaque as these crystals grew very rapidly along the sides of the glass container. Photographs 2 and 4 illustrate the difference in behaviour between two crystals mounted on different faces but grown under the same conditions of bulk supercooling; the crystal mounted on the fast growing (001) face producing fewer needle-like growths than one mounted on the slow growing (010) face. Through the temperature range of 37°C to 20°C, increase of supercooling produced a corresponding increase of the density with which such growths appeared on the surface of the innoculating seed.

Crystals grown rapidly at these large supercoolings were relatively opaque and therefore not quite suitable for conclusive microscopic examination under polarised light. Nevertheless, examination as before of some of these needle-like growths formed around 37°C indicated that the crystallographic orientation of these growths were different from that of the innoculating seed and from one another.

2.7 Innoculation of a supercooled benzophenone melt with pre-treated seed crystals

Following the above work it was found that if the crystal was pre-treated for some time at very low supercooling ($\Delta T \ll 1^{\circ}C$),

then subsequent immersion in a melt at high supercooling gave rise to results quite different from those described in section 2.5.

Pre-treatment or the 'healing' of the surface of the innoculating benzophenone seed crystal was effected by holding a crystal suitably mounted above the melt at 47°C ($\Delta T = 1°C$) for 10 minutes to allow the crystal to warm up, followed by 10 minutes immersion in the melt to permit some growth and then withdrawal to a position just above the melt for approximately 10 minutes to ensure solidification of all traces of the melt adhering to the crystal surface. The crystal with its surface so healed was quickly transferred to a position above another melt, under the test experimental conditions.

Innoculation of a supercooled benzophenone melt with a seed crystal treated in this manner resulted in the growth of the seed as a single crystal. Photographs 5 and 6 are those of a crystal with a pre-treated surface growing as a single crystal from a melt supercooled 21.5°C, and illustrates the absence of the phenomenon of breeding under these conditions of growth.

2.8 Discussion

These experiments show that the breeding of new crystals by the innoculation of supercooled benzophenone melts is almost certainly due to the presence of microcrystalline particles or dusts on the surface of the seed. These crystallites which do not form an integral part of the parent benzophenone seed crystal are responsible for the production of the crystals found floating on the surface of the melt as well as the needle-like growths observed on the crystal surface at higher supercoolings. These particles must have a wide spectrum of sizes as the number of these needle growths increases with the degree of supercooling at innoculation.

Working in aqueous solutions Mason[4] observed a similar phenomenon, where breeding was due to the presence of microcrystalline dusts on the surface of freshly added crystals; but he also observed other mechanisms which enabled the breeding process to continue after the original dust particles had falled off: these latter mechanisms were not observed in the present work with melts.

Crystals heated so as to eliminate surface contamination grow from melts at high supercoolings as single crystals and cause no breeding.

CHAPTER 3

GROWTH RATES OF SINGLE FREE GROWING CRYSTALS FROM STIRRED AND UNSTIRRED MELTS

3.1 Introduction

Experiments are described in this chapter in which the growth rates of benzophenone and salol crystals were determined while suspended on glass rods, under both stirred and unstirred conditions in the supercooled melt.

Rates of growth from the melt (ref. 20) of various crystals are given in the table below. The relatively extremely low rates reported for benzophenone and salol suggest that they are specially suitable substances for this research where it is desired that the growth process be as far as possible surface reaction controlled.

Substance	Supercooling (°C)	Maximum crystallisation Velocity (mm/min)
Naphthalene	-	∞ (spontaneous crystallisation)
Cyclohexane	-	∞ (" ")
Carbon tetrachloride	2-7	∞
Acetone	9-24	∞
p - dibromo benzene	27	7500
1,3,5 trichloro benzene	25	7000
Benzophenone	27.7	60
Salol	21.7	4.25

3.2 Benzophenone (001) face, unstirred melts

a) Experimental:- The displacement of a crystal face normal to itself was observed by following the crystal profile through the cross-wires of a cathetometer fitted with a vernier scale graduated in divisions of 10^{-3}cm. The growth rate was the slope of the resulting displacement-time plot.

By rotating the eyepiece of the cathetometer telescope, which was fitted with a polaroid disc, and by determining whether the crystal under observation had a single extinction angle or not for transmitted light, it was possible to say if the profile under observation was that of a single crystal.

Growth rate determinations were made with approximately 75 ml of the melt contained in a 100 ml erlenmeyer flask, which in turn was immersed in the constant temperature bath described in section 2.1. At the end of each run the melt was regenerated for use by heating this flask in a boiling water bath for about 5 minutes.

The rubber bung which stoppered the mouth of the flask had three holes drilled in it to introduce the stirrer, the crystal mounting and the thermocouple wires. A glass sleeve was also fixed between the stirrer and the bung to permit free rotation for the stirrer.

The surfaces of the crystals on which rate measurements were made, were first treated by a process of slow growth at 47.0°C ($\Delta T = 1^{\circ}C$), as described in section 2.5, to eliminate the possibility of 'breeding' and the complicated heat effects arising therefrom. The crystal was then lowered on its mount into a melt at the required degree of supercooling, and clamped when in position to insure against any accidental movement.

All measurements were made on the small fast growing (001) face of the benzophenone seed crystal (see figure 2), growing downwards into a melt, purified as in section 2.2, and mounted on a glass spike with its z - crystallographic axis in the vertical phane. This face was selected for study as it was identifiably different from the other faces of the crystal and because it had a measurable growth rate throughout the experimental range of supercoolings.

The duration of each run varied from approximately 15 minutes for determinations at large supercoolings, to 2 - 3 hours for runs of supercoolings of 1°C or less and the total displacement observed on the (001) face varied from about 0.3cm. to a maximum of about 2 cm.

b) Results:- Growth rate measurements on the (001) crystallographic face of the benzophenone crystal growing under these conditions are

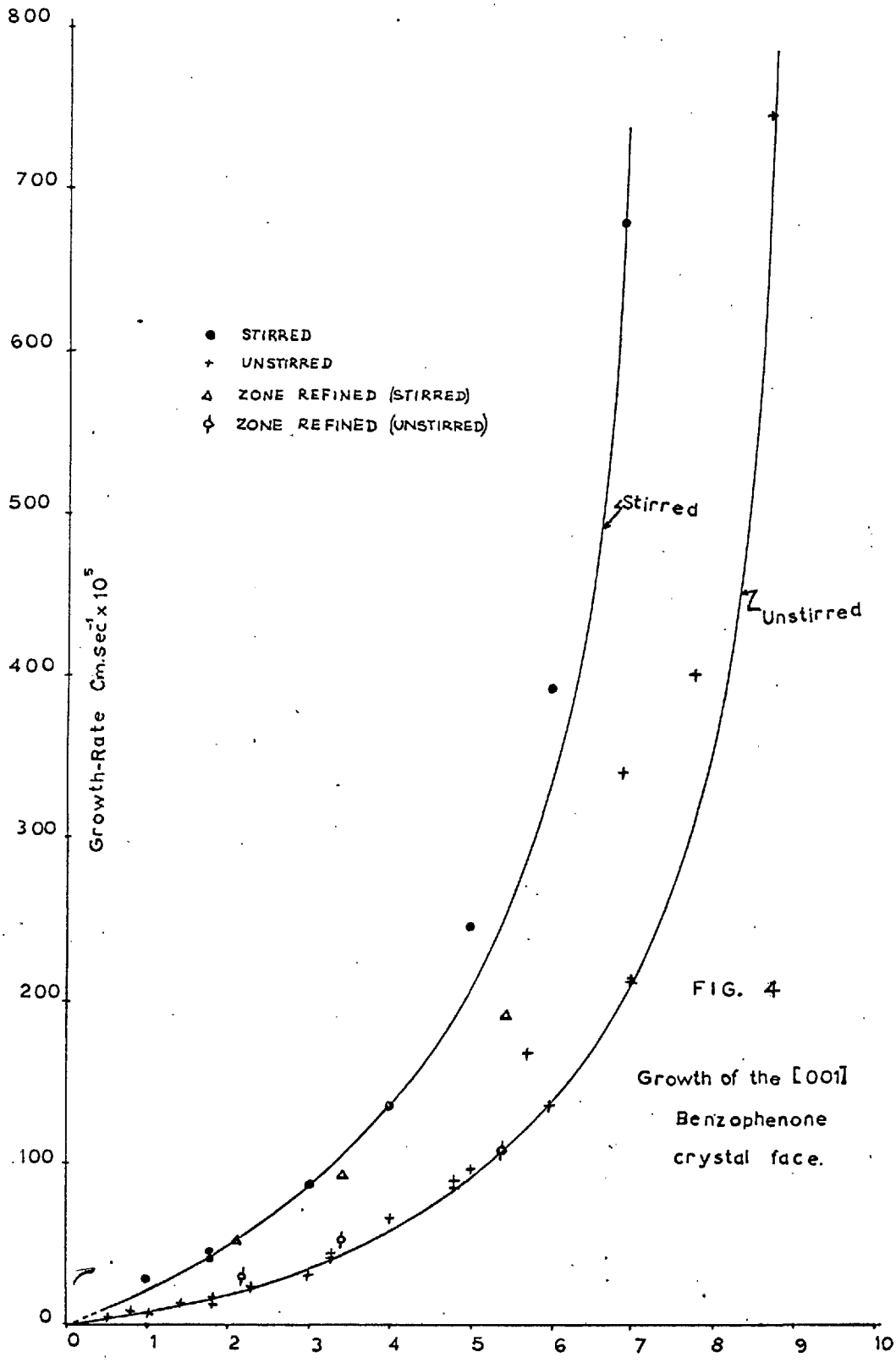

FIG. 4

Growth of the [001] Benzophenone crystal face.

tabulated in table 1, Appendix I, as a function of the supercooling in the bulk of the melt, and are illustrated by figure 4. Statistical analysis of these results for unstirred growths lead to the empirical equation $R_n = (5.88 \pm 1.12) \times 10^{-5} (\Delta T)^{1.80 \pm 0.28}$ cm/sec, with a correlation coefficient of + 0.94.

3.3 Benzophenone (001) face, stirred melts

a) Experimental:- In each of these determinations a 'treated' seed crystal was lowered into a melt supercooled to a preselected degree and allowed to grow for approximately 15 minutes under unstirred conditions before the crystal was spun. This allowed the crystal to grow firmly over the crystal mounting providing a better mechanical support, and also allowed sufficient time in which to make a determination of the unstirred growth rates, for subsequent direct comparison.

Agitation was provided by rotating the crystal on its mount at speeds ranging from 10 r.p.m. to a maximum of about 150 r.p.m. In the experimental range of supercoolings, a 2 or 3 fold increase of growth rate, over that of the unstirred growth rate under the same bulk supercooling, was observed on spinning the crystal at 48 - 50 r.p.m. but further increase of the rate of rotation did not produce

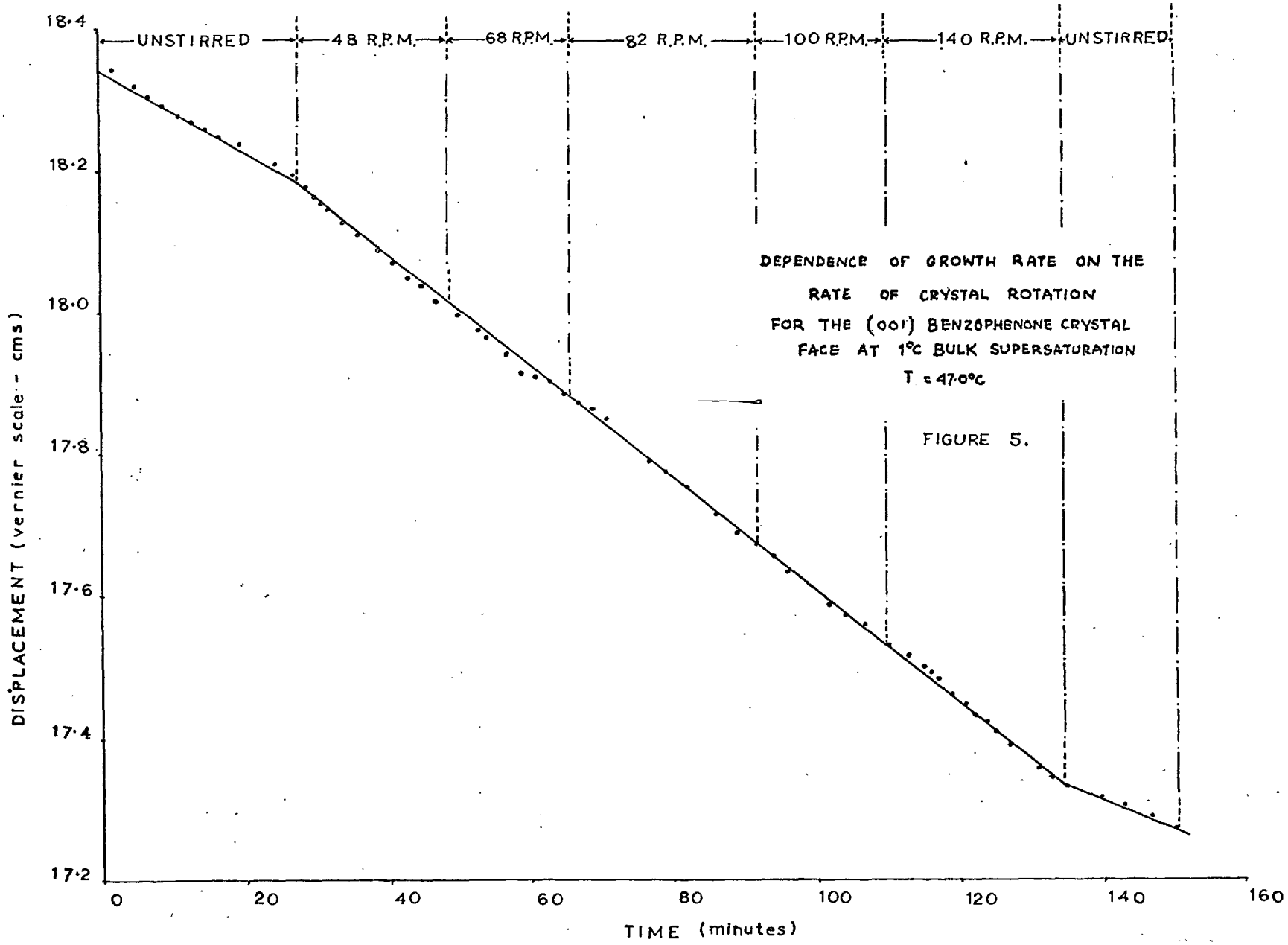

DEPENDENCE OF GROWTH RATE ON THE RATE OF CRYSTAL ROTATION FOR THE (001) BENZOPHENONE CRYSTAL FACE AT 1°C BULK SUPERSATURATION $T_s = 47.0°C$

FIGURE 5.

a corresponding increase in the growth rate. Figure 5 which is a displacement-time plot illustrates this effect for growth at 47.0°C, i.e. 1 deg C supercooling.

Agitation of the melt with an independent double-bladed stirrer, $2\frac{1}{4}$ cm from tip to tip rotating at 650 r.p.m., produced the same increase of growth rate as observed on stirring the crystal at 48 r.p.m. in the stagnant melt. Stirring the melt with the paddle rotating at 650 r.p.m., as opposed to rotating the crystal at 50 - 150 r.p.m., produced a marked increase of the tendency to nucleate elsewhere in the melt, limiting the time of observation to the time lag before new crystal nuclei were observed. Consequently, the rotating crystal method of providing agitation was selected for further work on benzophenone.

b) Results:- Rate determinations for stirred runs are tabulated in table 1, Appendix I and are also illustrated by figure 4. As with the unstirred runs, the growth rates were found to increase very rapidly with supercooling and a statistical analysis leads to an empirical relation of the form $R_u = (2.18 \pm 0.77) \times 10^{-4} (\Delta T)^{1.57 \pm 0.33}$ $cm.sec^{-1}$ with a correlation coefficient of + 0.97, for the kinetics of the surface reaction controlled mechanism of growth.

3.4 Zone refined benzophenone

a) Introduction:- As already explained the increased growth rate observed on stirring could be due to an increased value of the heat transfer coefficient. But it appeared also to be possible that the difference might be due in part at least to the presence of impurities in the melt: if these impurities were capable of reducing the surface growth rate, the retarding effect would be greater in the unstirred case. An attempt was therefore made to purify the melt even further by a process of zone-refining.

b) Experimental:- A sample of benzophenone, purified by double distillation as described in section 2.3, was placed in a porcelain boat 9cm in length, and drawn through a horizontal pyrex tube $3\frac{1}{4}$cm in diameter at a speed of 1cm/hour. A melted zone of approximately 2cm width was maintained electrically in this boat, with the aid of a nichrome wire heater wound round the pyrex tube. Each specimen of benzophenone was passed twice through the tube, in the same direction. A plug of benzophenone at the leading edge of the boat served as the centre initiating growth at the start of each pass through the heated section of the tube. The benzophenone used for the subsequent experiments was taken from the centre of the porcelain boat, the material 2cm from either end being rejected. This material melted

in a capillary at 48.0°C.

Rate measurements were made with the zone-refined benzophenone in a tube 3cm diameter containing approximately 25 ml of the benzophenone melt. The seed crystals and the melt used in the surface 'healing' process were made with the zone-refined material, and the melt was regenerated at the end of each determination, as previously, by warming the tube with its contents in a boiling water bath for about 5 minutes.

c) Results and discussion:- The results are tabulated in table 2 of Appendix I and are plotted on figure 4 for a direct comparison with the runs on benzophenone purified by distillative methods alone. The reasonably close agreement of rates for the two samples under both stirred and unstirred conditions of the melt, leads to the inference that the observed differences are not due to the presence of impurities. It may therefore be inferred that they are due to heat transfer effects.

3.5 Salol (010) face, unstirred melts

a) Introduction:- At this stage a study was made of the growth characteristics of the large and consequently slow growing (010) face of a salol crystal. Its growth rate was considerably smaller than

that of the (001) benzophenone face under comparable bulk supercoolings and it therefore seemed possible that the resistance to growth due to heat transfer could be reduced to the extent where the kinetics of the surface reaction could be observed.

b) Experimental:- Salol was purified for experimental purposes from material supplied by Hopkins and Williams as a General Purpose Reagent, by filtering its superheated melt through a Whatman No 1 paper followed by two slow (overnight) recrystallisation operations from absolute ethyl alcohol. The product, after drying in a vacuum, melted at 42.0°C to a clear transparent liquid.

Seed crystals were prepared from salol purified in this manner by the method described in section 2.3 for the preparation of the benzophenone seed crystals. The only modifications to this technique were that the seed crystals were developed by immersion in a melt at 32 - 33°C, and mounted for use by touching the (100) face with a warm glass spike. As observed with the benzophenone crystals, the large (slow growing) faces were unsuitable for mounting, when the seed was subsequently required to grow as a single crystal.

The surfaces of these crystals, mounted on a glass spike, were then 'healed' by re-immersion in a melt at 40.5°C ($\Delta T = 1.5°C$) for

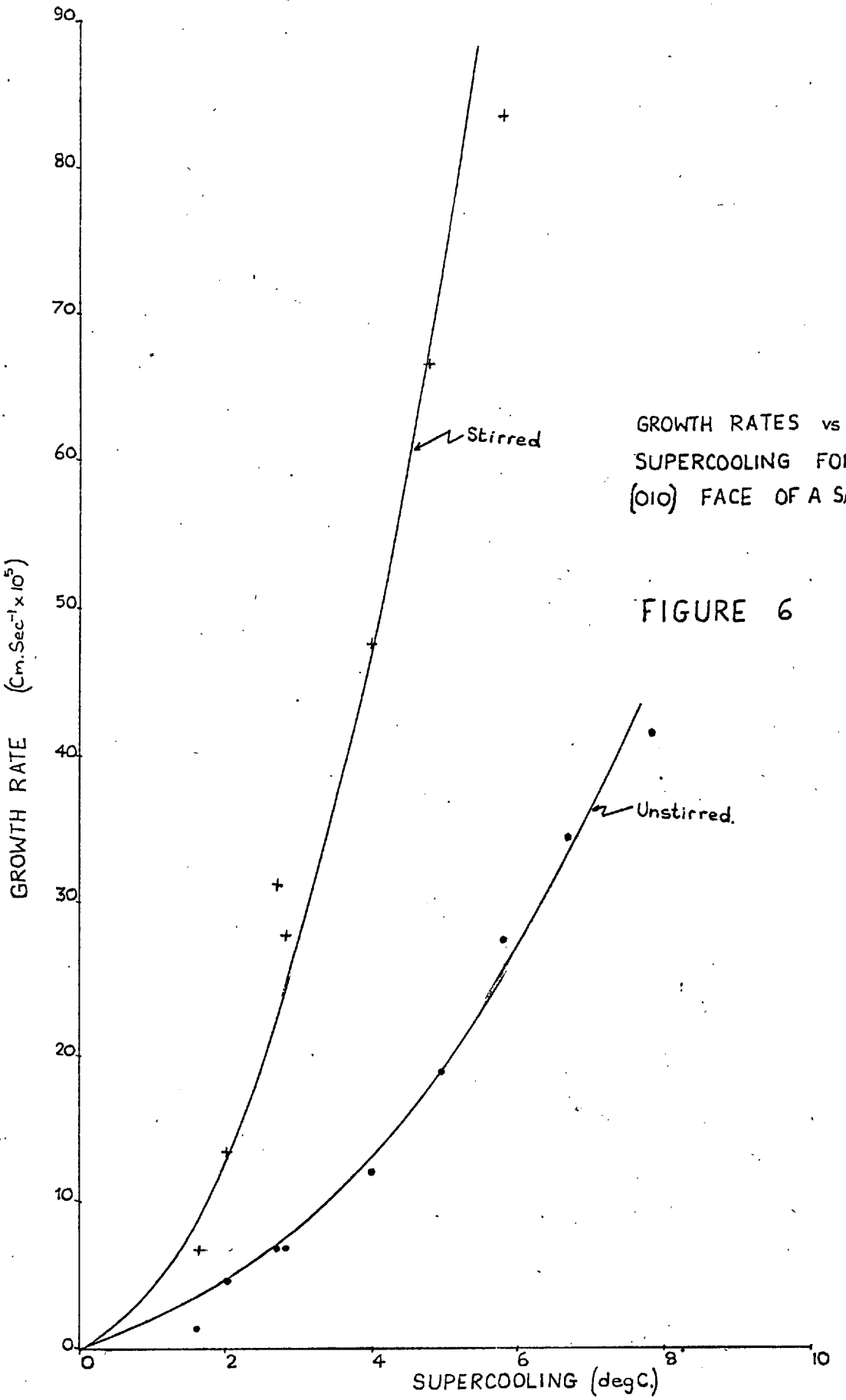

GROWTH RATES vs BULK SUPERCOOLING FOR THE (010) FACE OF A SALOL CRYSTAL.

FIGURE 6

approximately 15 minutes, in the manner described in section 2.4 for healing seed crystals of benzophenone, and lowered on its mount into the melt at the required degree of supercooling. The bulk supersaturation was kept constant for the duration of each run, but several runs were made in the temperature range 40.4°C to 34.2°C (ΔT = 1.6 to 7.8°C), using a different seed crystal for each determination.

Displacement measurements were made on the slow growing (010) face of a salol crystal growing horizontally, i.e. with the z - crystallographic axis vertical. The melt was contained in an erlenmeyer flask, which in turn was immersed in a constant temperature water bath, as in the experiments previously described.

The duration of each experiment varied from about three hours for the runs with supercoolings of less than 2°C, decreasing progressively with increase of supercooling until periods of approximately 10 minutes were employed for growth from melts whose bulk supercooling was in excess of 6 deg C. In this period of time the displacement observed on the (010) face ranged from 0.2cm to about 0.6cm.

c) Results:- The results of these experiments which are tabulated in table 3 and plotted on figure 6, illustrate that the growth rates increase more than linearly with supercooling and that they were

approximately 8 - 10 times slower than that of the (001) benzophenone face growing from an unstirred melt under the same bulk supercooling.

3.6 Salol (010) face, stirred melts

a) Introduction:- Once these rates from unstirred melts were determined, the rates of growth from well stirred melts were required, as before, to establish the relative importance of the heat transfer process in governing overall kinetics.

b) Experimental:- The experimental procedure was identical to that employed for the rate determinations from unstirred melts, except for the agitation of the melt which was provided with a double-bladed propellor described in section 3.3. The crystal was kept stationary and held in position by clamping the glass mount. The stirrer was positioned so as to keep the tip of the propellor out of contact with the crystal, generally 1 - 2cm away from the crystal edge at nearest approach. The propellor was rotated at approximately 650 r.p.m., and this ensured the maximum agitation possible for this system, without actually sucking in air into the melt.

c) Results:- Agitation of the melt produced a 4 to 5 fold increase in growth rate over that of the unstirred rate, and these results are

also tabulated in table 3 and are illustrated in figure 6. In the determinations from the melts whose supercoolings were 3 deg C and below, increase in the rate of stirring from 400 to 650 r.p.m. produced no detectable change in growth rate, but the figures quoted for the runs whose bulk supercoolings were in excess of 4 deg C are those observed only at the highest rates of stirring. It is therefore possible that the heat transfer effects have not been altogether eliminated from the runs with supercoolings of more than 4 deg C. The experimental range of observation could not be extended beyond 6 deg C supercooling, ($36^{\circ}C$), due to limitations imposed by the tendency to 'breed' new crystal nuclei, under these conditions of very high agitation.

3.7 Salol (100) face, unstirred melts

a) Introduction:- These experiments were conducted with a view to determining the growth characteristics of the fast growing (100) face of a freely growing crystal of salol from unstirred melts, and subsequently to compare these with the capillary growth rates (see Chapter 6).

b) Experimental and Results:- The experimental procedure adopted was identical to that described in section 3.5 for the determination

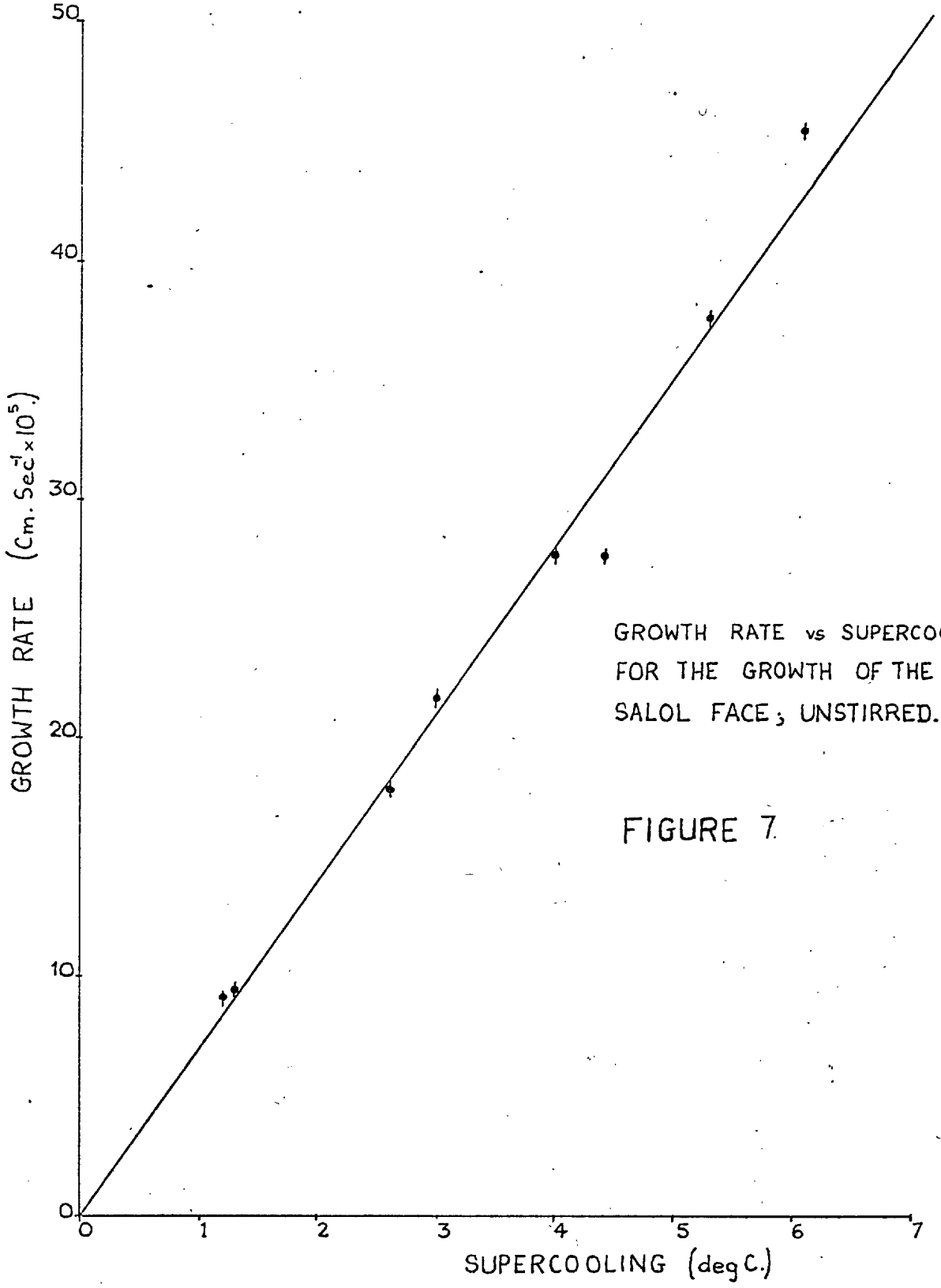

GROWTH RATE vs SUPERCOOLING FOR THE GROWTH OF THE (100) SALOL FACE; UNSTIRRED.

FIGURE 7.

of the unstirred rate of the (010) face.

The results which are tabulated in table 4 of Appendix I and illustrated by figure 7, show an approximate linear increase of rate with supercooling. In this respect it differs from the unstirred growth characteristics of both the (001) benzophenone face and of the (010) salol face.

3.8 Summary

The growth characteristics of the (001) face of a benzophenone crystal have been studied as a function of the bulk supercooling in both unstirred and stirred melts, and empirical equations have been derived to describe their interdependence.

Impurities have been ruled out as a possible cause for the differences in rate between the stirred and unstirred runs as zone refinement of the sample of benzophenone had no effect on either rate. It must therefore follow that these differences in rate were due to heat transfer effects, despite the very low growth rates.

Rate measurements made on the slow growing (010) face of a salol crystal show a similar difference in rate between stirred and unstirred growth runs. Consequently these rates must also be

controlled to a considerable extent by heat transfer. However, if heat transfer was important, it would be difficult to see how these rates could increase more than linearly with bulk supercooling.

A brief description is also given of the growth kinetics of the fast growing (100) face of the salol crystal from unstirred melts.

3.9 Conclusions

a) The stirred rate of growth is very much larger than the unstirred. Therefore, heat transfer is important.

b) The increase of the heat transfer due to natural convection is sometimes considered to vary as $(\Delta T)^{1.25}$, whereas the unstirred rate of growth of the benzophenone face is a function of $(\Delta T)^{1.8}$.

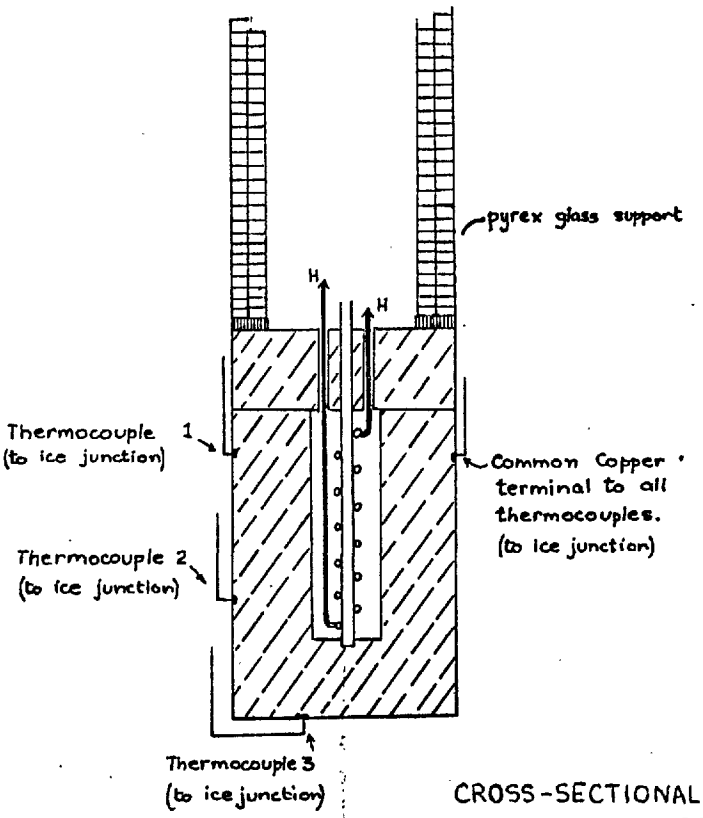

CROSS-SECTIONAL SKETCH OF COPPER VESSEL.

FIGURE 8

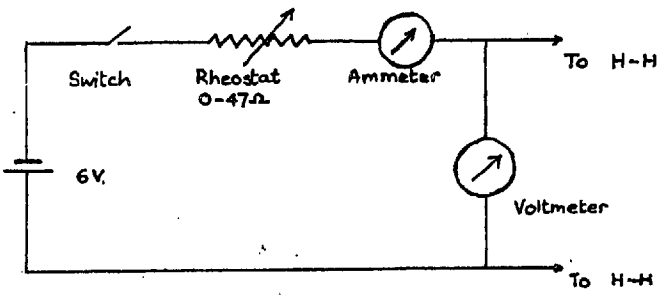

ELECTRICAL CIRCUIT FOR NICHROME HEATER

FIGURE 9.

CHAPTER 4

DIRECT MEASUREMENT OF HEAT TRANSFER COEFFICIENTS

4.1 Introduction

In view of the conclusions at the end of the preceding chapter it appeared desirable to try to measure the heat transfer coefficients in benzophenone and salol melts by a direct and independent method.

4.2 Apparatus

These direct measurements of the coefficient of heat transfer, h, were made with an electrically heated copper vessel of height 1.6 cm, diameter 0.95cm and wall thickness 0.32cm (see figure 8). A 6.8ohm coil of nichrome heating wire was wound round a pyrex capillary tube in the central cavity of this vessel, to which current was supplied from a variable current source (see figure 9), by means of two copper wires of negligible internal resistance.

40-gauge constantan thermocouple wires were soldered onto the external surface of the copper vessel to enable the thermoelectric e.m.f. generated between this junction and another in melting ice to be recorded with the use of a Pye precision potentiometer reading to a microvolt. A null deflection method of recording was employed with a Pye suspended coil microvoltmeter. The vessel itself functioned as the common copper component of each thermocouple junction.

The copper vessel was held in position by clamping the supporting pyrex glass tube, which in turn was fastened to its upper surface with araldite, and the measurements were taken while it was totally immersed in the melt contained in a 100 ml erlenmeyer flask. Heat losses from the upper surface of the pot were neglected under steady state conditions as the thermal conductivity of copper (1.03 g.cal.sec^{-1}. cm^{-2} $^{o}C^{-1}$.cm) exceeded by far that of pyrex glass (0.0026 g.cal. sec^{-1}. cm^{-2} $^{o}C^{-1}$.cm).

Heat transfer coefficients at the copper-melt interface were determined by measuring the energy supplied to the heater and the corresponding rise in temperature at the surface of the copper vessel. All the coefficients given in the text will be understood to be in cal.cm^{-2} sec^{-1} $^{o}C^{-1}$.

4.3 Unstirred benzophenone (fast growing (001) face)

The coefficient of heat transfer from a copper surface into unstirred benzophenone melts increased from 2.67×10^{-3} for an interfacial difference of 2.4°C to 4.93×10^{-3} for a temperature drop of 16.7°C in an approximately linear manner. In each of these determinations the temperature in the bulk of the melt was maintained at 48.0°C. Results are tabulated in table 5 of Appendix I and are

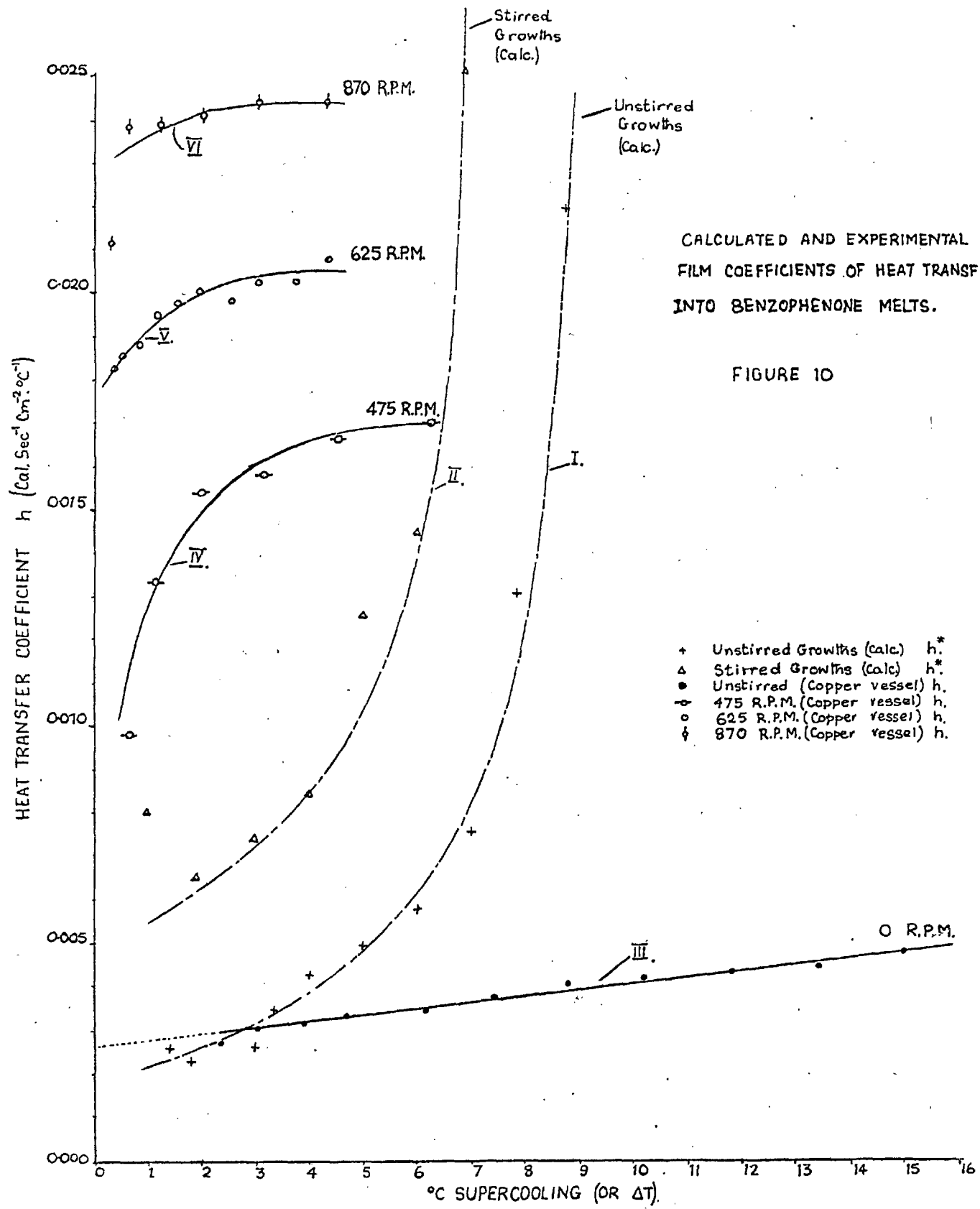

CALCULATED AND EXPERIMENTAL FILM COEFFICIENTS OF HEAT TRANSF INTO BENZOPHENONE MELTS.

FIGURE 10

illustrated by curve III in figure 10.

The measured film coefficients, h, are compared with the coefficients h^* (curve I), which would be required to account for the observed rates of growth of the fast growing (001) face of the benzophenone crystal, assuming that these growth rates were wholly heat transfer controlled, i.e. h^* is defined by

$$h^* = \frac{\text{observed rate of growth} \times \rho \lambda}{T_m - T}$$

where $T_m - T$ is the overall supercooling.

It will be seen that the value of h varies only slightly with supercooling, as would be expected. On the other hand the curve of h^* varies as a steep function of ΔT: and in fact the h^* curve crosses the h curve at about $\Delta T = 3$ and increases so rapidly that at $\Delta T = 9$ the value of h^* is over 5 times that of h. This result is altogether surprising since it would at first sight appear that h should always be less than h^*, and that h would only become equal to h^* in the limiting case of complete heat transfer control. A possible explanation however is that a part of the heat generated by deposition of material on this fast growing face is conducted away into the crystal and dissipated into the melt through the slower growing faces.

That some heat can be transferred in this manner was abundantly confirmed by the thermocouple experiments which will be described in section 5.2. It is however still difficult to understand how such a large amount of heat could be dissipated in this way, and some further explanation is still being sought.

4.4 Stirred benzophenone (fast growing (001) face)

The melt was agitated with the stirrer described in section 3.3 and the coefficients of heat transfer, h, were determined experimentally for stirring speeds of 475, 625 and 870 r.p.m.

These results are tabulated in table 5 and shown in figure 10 curves IV - VI, together with the values of h^* (see table 6, curve II) defined above but based in this case on growth-rates from melts with the crystal rotated at 48-50 r.p.m.

The values of h are much greater than in the case of unstirred melts, and are seen to increase rapidly with stirring speed. These values of h were higher than those of h^* at low supercoolings, but for supercoolings above about 6.5°C the apparently anomalous situation in which $h^* > h$ was once again encountered. This again suggests that only a part of the heat generated by deposition of material on the (001)

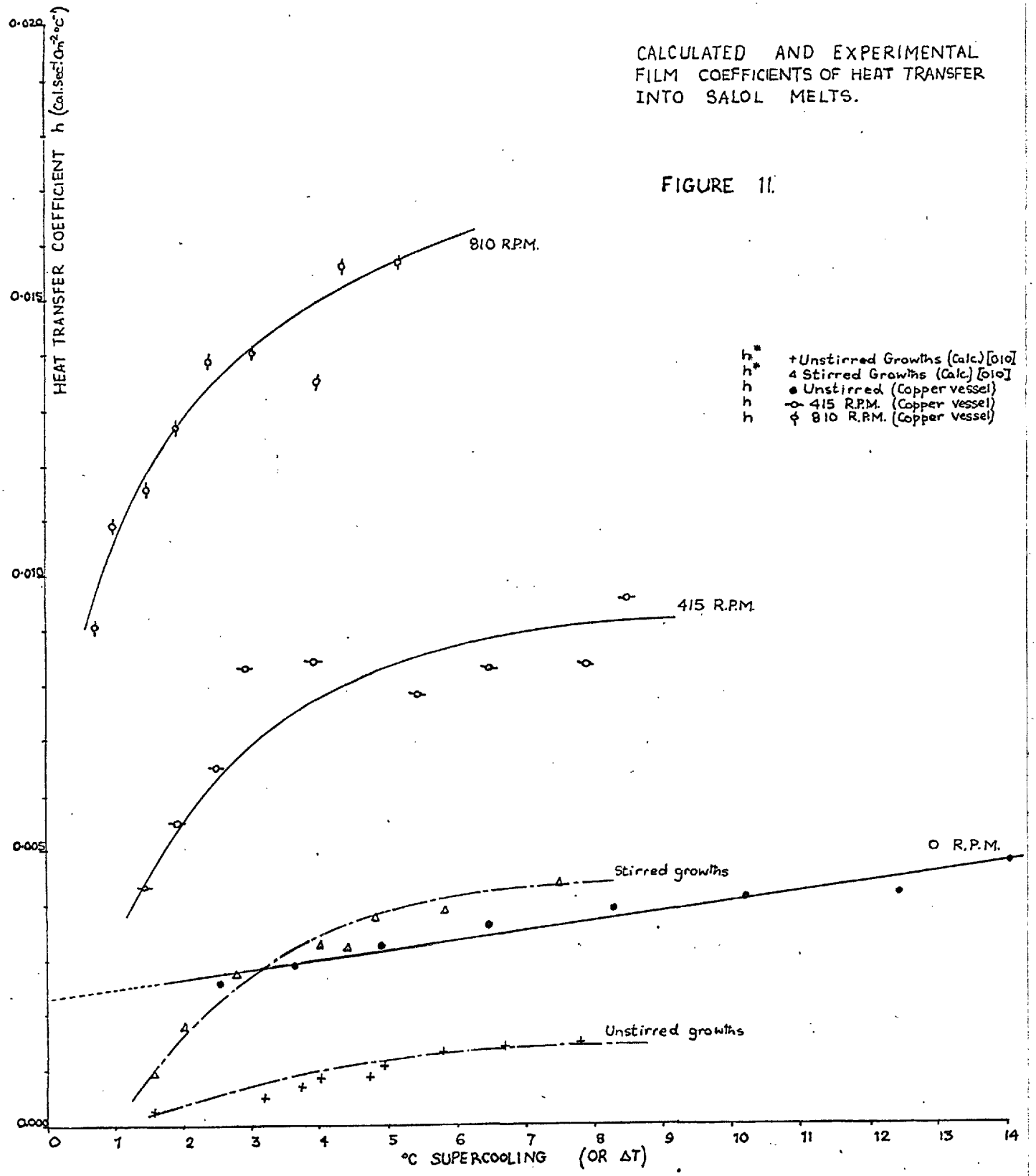
CALCULATED AND EXPERIMENTAL FILM COEFFICIENTS OF HEAT TRANSFER INTO SALOL MELTS.
FIGURE 11.
HEAT TRANSFER COEFFICIENT h (cal.sec⁻¹cm⁻²°c⁻¹)
0·020
0·015
0·010
0·005
0·000
h* +Unstirred Growths (Calc.) [010]
h* 4 Stirred Growths (Calc.) [010]
h • Unstirred (Copper vessel)
h -o- 415 R.P.M. (Copper vessel)
h ϕ 810 R.P.M. (Copper vessel)
810 R.P.M.
415 R.P.M.
0 R.P.M.
Stirred growths
Unstirred growths
0 1 2 3 4 5 6 7 8 9 10 11 12 13 14
°C SUPERCOOLING (OR ΔT)

face could be dissipated across the interface, even in well stirred melts, and the remainder must be conducted away from the crystal surface through the solid.

4.5 Unstirred salol (slow growing (C10) face)

The coefficients of heat transfer from the surface of the copper vessel into unstirred melts of salol were determined in the manner described in sections 4.2 and 4.3; the temperature in the bulk of the melt being held at 42.0°C.

The heat transfer coefficient so determined increased from 2.64×10^{-3} for a temperature drop of 2.6 deg C across the interface to 3.02×10^{-3} for a difference of 16.2 deg C in an approximately linear manner (see figure 11, table 7). These values being almost identical with the corresponding results with benzophenone.

The corresponding values for the coefficient h^* (figure 11, table 8) for the (010) face of salol ranged from 0.203×10^{-3} at 1.6 deg C supercooling to 1.44×10^{-3} for a growth rate of 4.12×10^{-4} cm.sec^{-1} corresponding to a bulk supercooling of 7.8 deg C. These values are considerably lower than those determined experimentally for the heat transfer coefficients, (h), and compatible with a

mechanism which is partly controlled by heat transfer and partly by the surface reaction.

The heat transfer coefficient determined by the thermocouple technique to be described in Chapter 5, from direct measurement of temperatures at the (010) surface of a growing crystal of salol was 2.50×10^{-3} for temperature differences upto 3.5 deg C. This is in very good agreement with the experimental values (h) stated above; and this would appear to provide mutual confirmation of the validity of the thermocouple technique and the copper pot technique. The continuous increase of temperature observed even after the thermocouple has been completely enveloped by the slow growing (010) face, though not with the relatively fast growing (100) face, confirms the deduction made on the fast growing face of the benzophenone crystal that a part of the heat generated on the fast growing face is dissipated into the melt through a slower growing face.

4.6 Stirred salol (slow growing (010) face)

These coefficients of heat transfer from the copper surface into agitated salol melts were determined at stirring speeds of 415 r.p.m. and 810 r.p.m., described in section 4.4, but with a temperature of $42.0^{\circ}C$ in the bulk of the melt. The coefficients so determined were

once again found to increase with ΔT. They were of course strongly dependent on the rate of agitation (figure 11, table 7).

The values of the coefficient h^* are shown in figure 11 and table 3. These are considerably lower than the values of the experimental coefficient h, and so are compatible with an actual mechanism of growth governed partly by heat transfer and partly by surface reaction kinetics.

The heat transfer coefficients h determined by the thermocouple technique, which will be described in the following Chapter, were not constant with ΔT, but increased in a random manner, and ranged from 4.56×10^{-3} to 17.1×10^{-3}. These measurements were made at a supposedly constant stirring rate of 450 r.p.m., but the wide variations in the heat transfer coefficients are possibly to be ascribed to the fact that the crystals were not always mounted in a constant position with respect to the stirrer. Despite this haphazard variation, these values are quite comparable in magnitude with those determined by the copper pot technique, with a stirring speed of 415 r.p.m. (table 7).

4.7 Summary

The rates of growth from unstirred melts observed on the (001) face of the benzophenone crystal are higher than would be permitted by the rates of heat transfer observed in the copper pot. This may be explained by assuming that a part of the heat generated on this face is conducted away and dissipated into the melt through a slower growing face.

The same is true for the growth of the (001) benzophenone face from the stirred melt at relatively high growth rates, corresponding to bulk supercoolings in excess of about $6.5^{\circ}C$.

Heat transfer coefficients determined with the copper vessel in unstirred melts of salol agreed very closely with those determined on the (010) face of a growing crystal with the use of thermocouple. This agreement tends to confirm the validity of the thermocouple technique and of the kinetic measurements derived therefrom.

In stirred melts the magnitude of the heat transfer coefficient determined with the thermocouples appeared to vary in a rather random manner but were of the same order of magnitude as those determined with the copper vessel, h.

The copper pot experiments on the whole tend to confirm the idea that resistance to growth is partly due to heat transfer limitations, which is operative in spite of the very low surface growth rate of salol. In addition, these experiments have emphasised the possibility of the transfer of heat through the crystal, and also the possibility of non-uniformity of temperatures of the crystal surface. The question was therefore pursued further with the thermocouple technique described in the following Chapter.

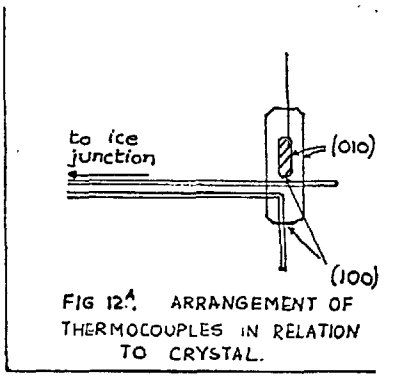

FIG 12A. ARRANGEMENT OF THERMOCOUPLES IN RELATION TO CRYSTAL.

TEMPERATURE PROFILE AT TWO CRYSTAL MELT INTERFACES OF A GROWING SALOL CRYSTAL.

T = 39·50°C

ΔT = 2·50°C.

FIGURE 12.

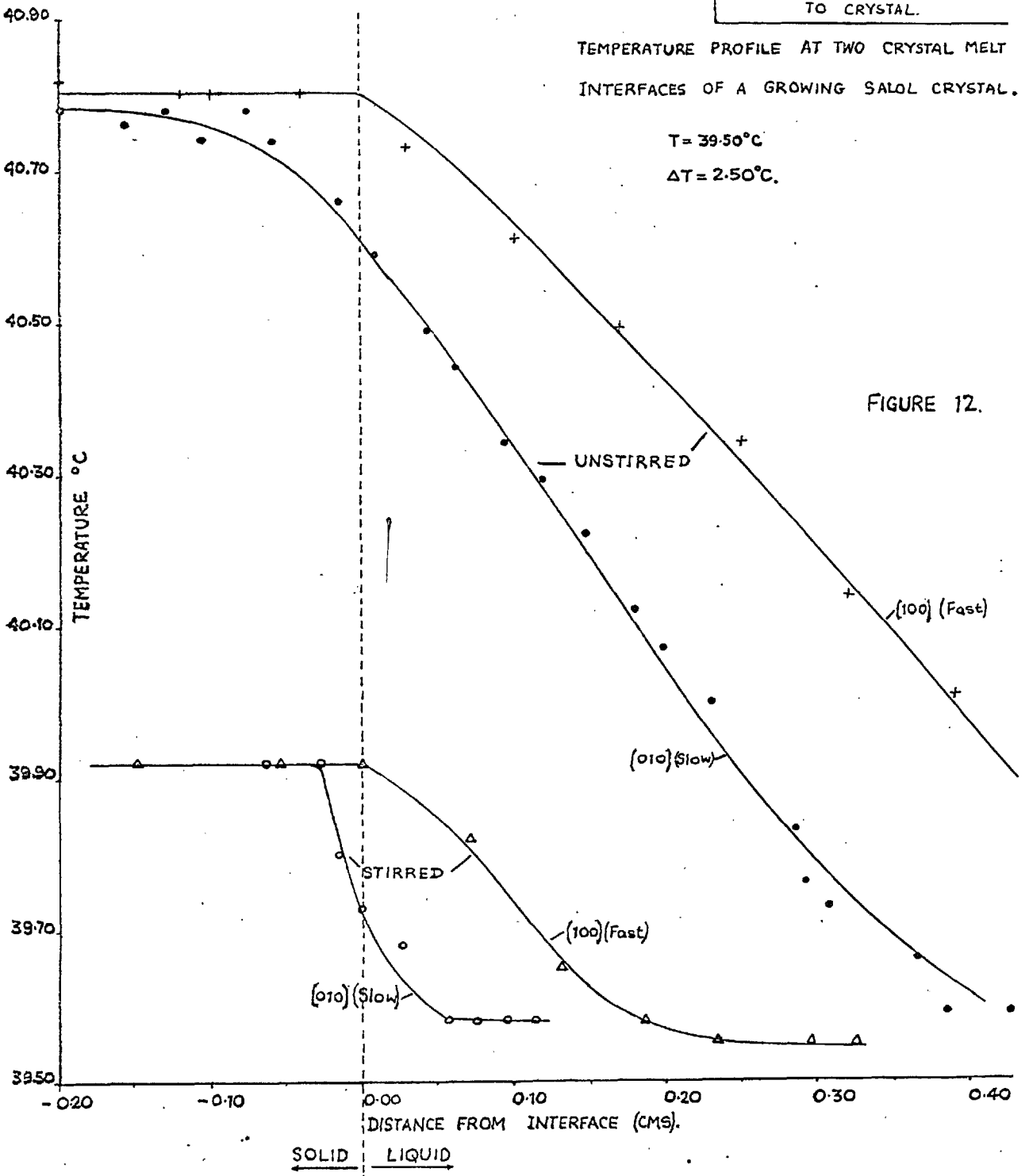

CHAPTER 5

THERMOCOUPLE TECHNIQUE OF MEASURING THE INTERFACIAL TEMPERATURE CHARACTERISTICS OF A FREE-GROWING SALOL CRYSTAL

5.1 Introduction

Experiments are described in this chapter in which the surface temperatures of a growing salol crystal are measured with thermocouples in both stirred and unstirred melts. The kinetics of the surface reaction are studied in this manner, free of the effects due to heat transfer, and many of the experimental results described in Chapters 3 and 4 are explained in the light of these findings.

5.2 Temperature characteristics at the (010) surface of a growing salol crystal

a) Experimental:- A crystal of salol mounted on a glass spike and with its surface treated as described in section 3.4, was lowered into an unstirred melt so that it was directly above the 40 gauge wires of two copper constantan thermocouples. The thermocouples were arranged in such a manner with respect to the crystal (see figure 12^{A}), that it subsequently grew over the thermocouples with the (010) face normal to one thermocouple and parallel to the other. This enabled the temperature profiles of both the slow growing (010) face and that of the relatively fast growing (100) face to be measured on the same crystal. The surface temperature of the crystal face was taken to be that recorded by the thermocouple as the crystal advanced over the

thermocouple junction and the distance of this crystal face from the junction was measured with the cathetometer. The growth rate was obtained from the slope of the resulting displacement-time plot.

The stirrer was switched on (at approximately 450 r.p.m.) for the stirred runs, only after the crystal had grown over both thermocouple wires in the stagnant melt. The technique of growing the crystal over the thermocouple wires and towards the junction had to be employed in preference to an alternative method of growing the crystal directly in front of the thermocouple junction, to avoid 'breeding' by attrition between the thermocouple and the crystal.

b) Results and discussion:- Figure 12 (see table 9), shows the temperature profile across the slow growing (010) crystal face as well as that of the (100) face of a crystal of salol growing from a melt under both stirred and unstirred conditions at 39.5°C, i.e. a bulk supercooling of 2.5 deg C.

This illustration which is typical of the temperature profiles show a continuous increase of temperature even after the (010) face completely envelopes the thermocouple junction. It also illustrates the non-uniformity of surface temperatures over different faces of the same crystal, from which it follows that the interfacial supercooling

would also vary from face to face. In this instance the interfacial supercooling available for the growth of the (100) face from an unstirred melt with a bulk supercooling of 2.5 deg C, was 1.2 deg C, while the supercooling at the (010) face was 1.4 deg C. The corresponding values for the stirred melt at the same bulk supercooling of 2.5 deg C were 2.1 and 2.3 deg C respectively.

The marked differences in the growth rate of the (010) salol face from unstirred and stirred melts described in sections 3.5 and 3.6, can now be explained on the basis of the widely different interfacial supercoolings available for growth while at the same bulk supercooling.

The apparantly anamalous situation which arose in sections 4.3 and 4.4 on the rates of growth of the (001) benzophenone crystal face from both unstirred and stirred melts when $h^{*} > h$, is now explained on the basis of experimental evidence for a mechanism whereby heat is conducted through the crystal. The existance of a temperature gradient within the crystal is made possible due to the non-uniformity of surface temperatures.

5.3 Growth rate as a function of true surface supercooling. Salol (010). Stirred and unstirred

a) Experimental:- The procedure adopted in measuring the temperature

THE EFFECT OF THE INTERFACIAL TEMPERATURE ON T
GROWTH RATE OF THE (010) FACE OF THE
SALOL CRYSTAL

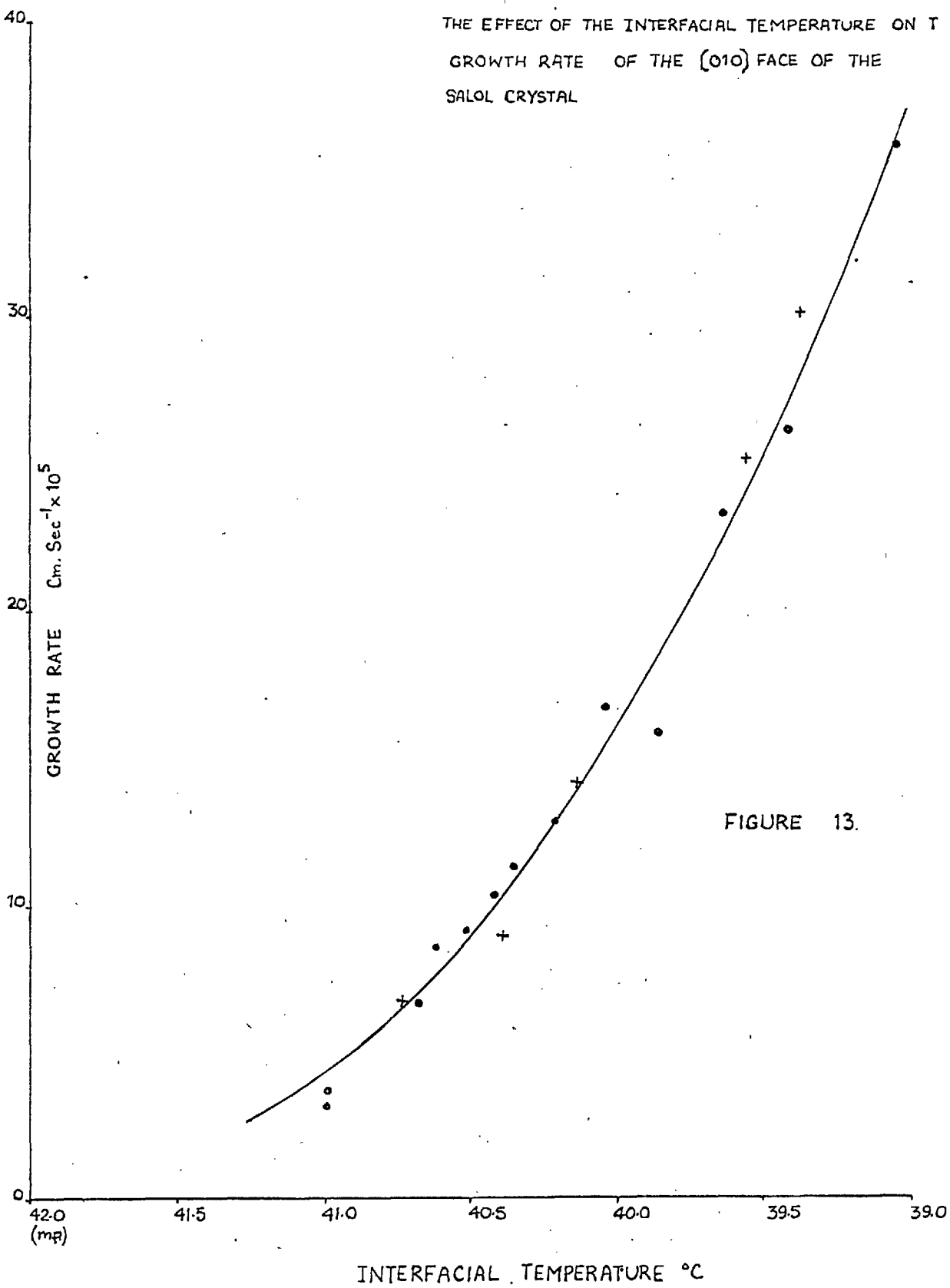

FIGURE 13.

at the crystal surface was similar to that described in section 5.2 and the growth rates were determined from displacement-time measurements as in section 3.5. In the stirred runs a stirring speed of approximately 450 r.p.m. was adopted and the rate determinations were made within a bulk supercooling range of 1.25 to 6.50 deg C (40.75 to 36.50°C).

b) Results and discussion:- Table 10 of Appendix I give growth rates as a function of the surface temperatures of the (010) face of salol crystal under both stirred and unstirred conditions in the melt. These results are illustrated in figure 13 in which growth rates are plotted against surface supercoolings for both stirred and unstirred melts. These rates are seen to be quite independent of whether the melt was stirred or not and to be functions only of the true surface supercoolings.

A statistical analysis of the results of the thermocouple experiments leads to an empirical result of the form $R_i = (3.66 \pm 0.48) \times 10^{-5} (\Delta T_i)^{2.06 \pm 0.14}$ $cm.sec^{-1}$ with a correlation coefficient of + 0.99, for the kinetics of the surface reaction mechanism of growth at the (010) salol face, in both stirred and unstirred melts.

These rates which give growth rates as a function of the temperature of the crystal face are believed to provide for the first

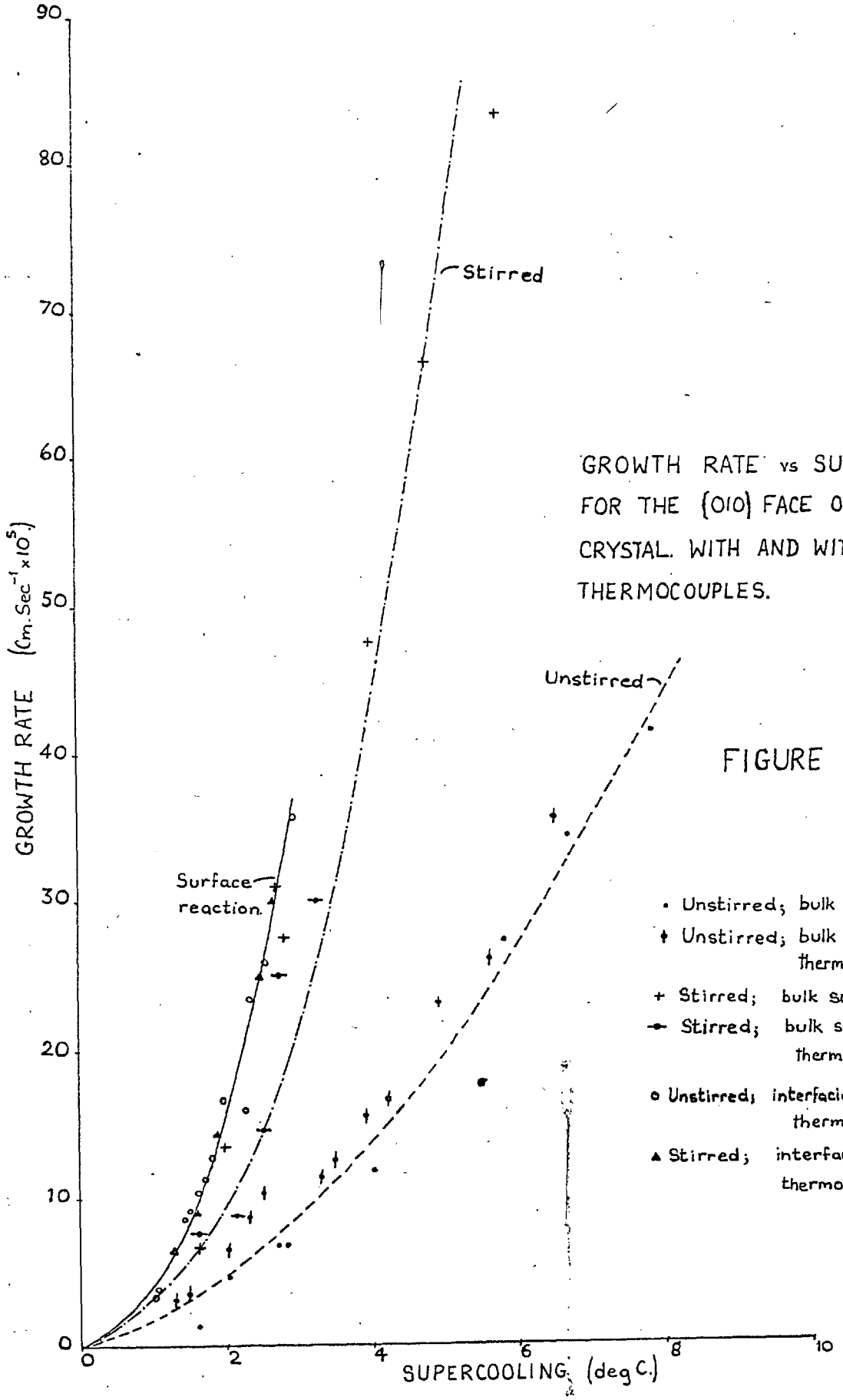

GROWTH RATE vs SUPERCOOLING FOR THE {010} FACE OF A SALOL CRYSTAL. WITH AND WITHOUT THERMOCOUPLES.

FIGURE 14.

- Unstirred; bulk supercooling.
- Unstirred; bulk supercooling; thermocouples present.
- Stirred; bulk supercooling.
- Stirred; bulk supercooling; thermocouples present.
- Unstirred; interfacial supercooling; thermocouples present.
- Stirred; interfacial supercooling; thermocouples present.

time the true kinetics of the surface reaction for the unrestricted growth of a crystal face from the melt.

Figure 14 compares the rates of growth of the (010) salol face

a) As a function of overall supercooling in unstirred melts (ex. table 3 and figure 6).

b) As a function of overall supercooling in stirred melts (ex. table 3 and figure 6).

c) As a function of the true surface supercooling in both stirred and unstirred melts (ex.table 10, figure 13).

The close agreement of rates with and without thermocouples present in both stirred and unstirred runs shows that the presence of thermocouples does not affect the rates of growth of the crystal face.

This comparison shows that the effects due to heat transfer have not been altogether eliminated from the stirred runs described in section 3.6 despite the low rates of growth ($10\text{-}90 \times 10^{-5}$ cm.sec^{-1}), coupled with the high stirring rates (650 r.p.m.). Nevertheless they have been substantially reduced; viz. at 3 deg C interfacial supercooling, the rate of growth determined by the true surface kinetics is approximately 35×10^{-5} cm.sec^{-1}, while the rates of the stirred and

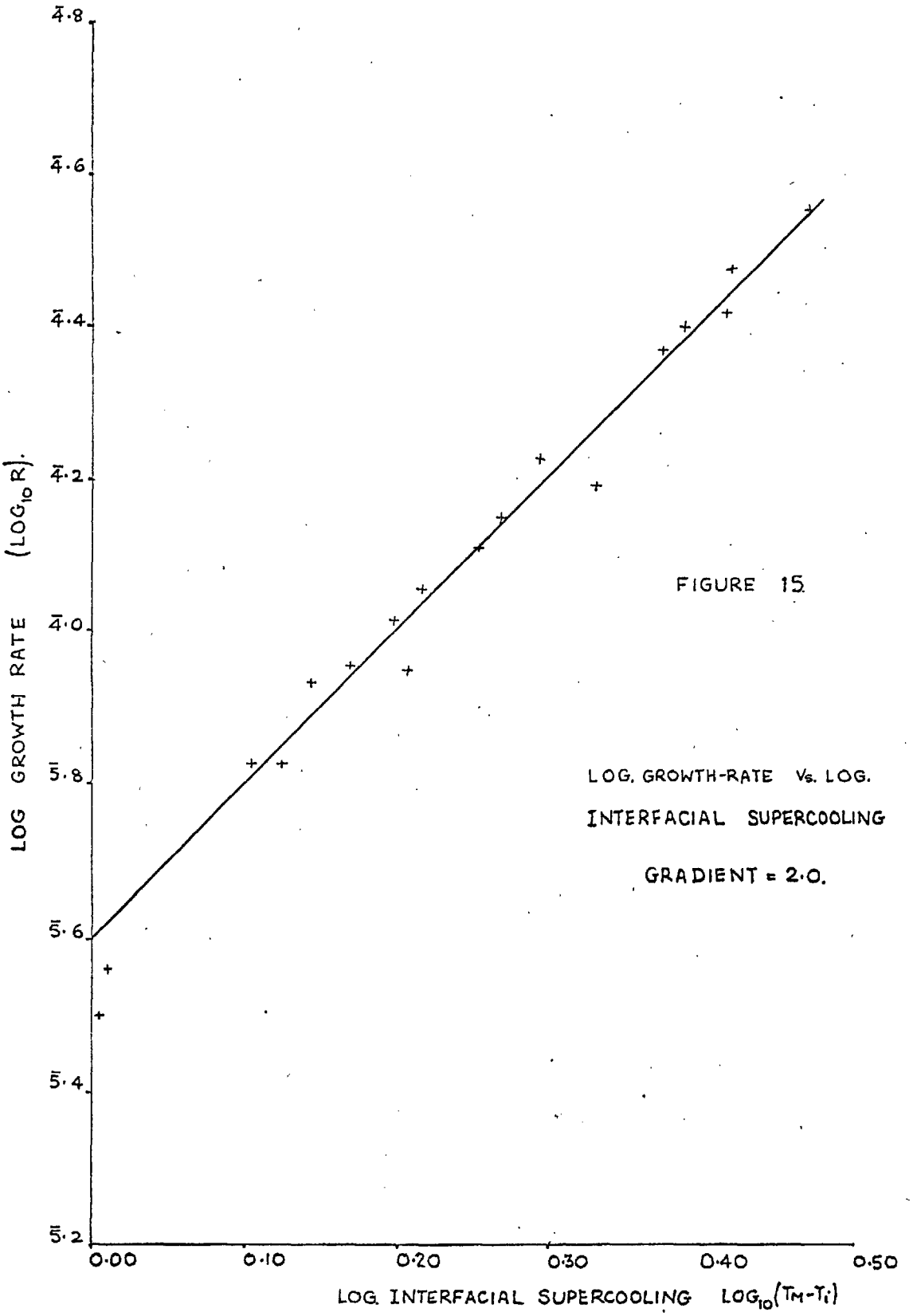

FIGURE 15.

LOG. GROWTH-RATE Vs. LOG. INTERFACIAL SUPERCOOLING

GRADIENT = 2·0.

GROWTH RATE vs. TEMPERATURE DRIVING FORCE
IN UNSTIRRED SALOL MELTS.

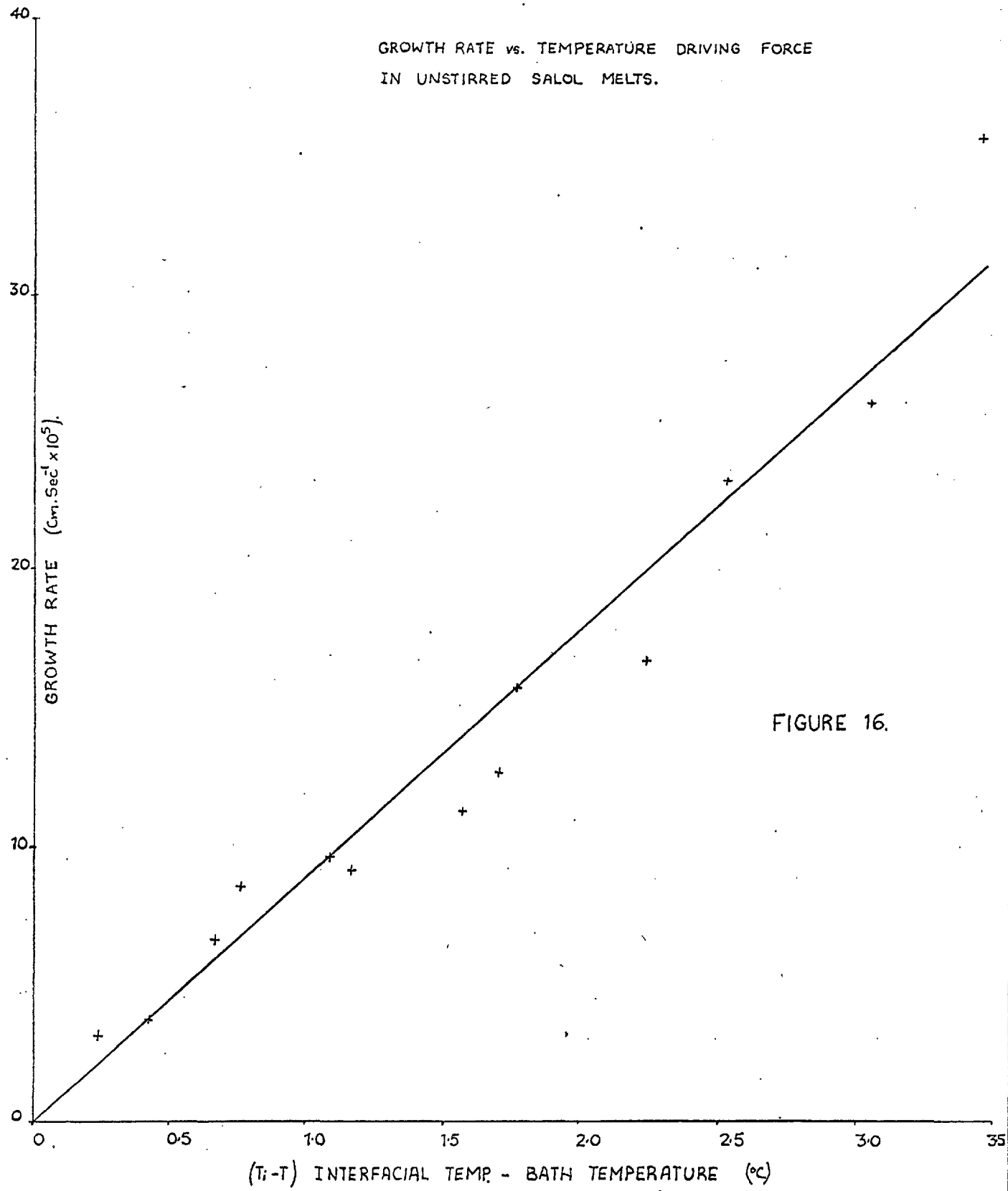

FIGURE 16.

unstirred runs at 3 deg C bulk supercooling are about 25 x 10^{-5} and 8 x 10^{-5} cm.sec^{-1} respectively.

5.4 Heat transfer coefficients

Coefficients for heat transfer between the crystal face and the melt were calculated on the basis that the thermal driving force was the difference between the interfacial temperature and that in the bulk of the melt, $(T_i - T)$. Figure 16 (table 10) illustrates the relation between $(T_i - T)$ and the rate of growth of the (010) salol face from an unstirred melt. The coefficient of heat transfer calculated from the slope of this plot was 2.50 x 10^{-3}, which compares with about 2.64 x 10^{-3} for the copper vessel.

These results and also those from the stirred melts have already been discussed in sections 4.5 and 4.6.

5.5 Summary

Non-uniformity of surface temperatures of a growing crystal explains the existance of temperature gradients within a crystal. This makes it possible for a part of the heat liberated on a fast growing face to be dissipated through a cooler and relatively slower growing face, and account for the observation that $h^* > h$.

The growth rates of the (010) salol face in a freely suspended crystal have been shown to be dependent on the interfacial temperatures alone, and otherwise independent of whether the melt was agitated or not. The true kinetics of the surface reaction determined by this thermocouple technique explain rather well the divergence of the observed rates in the stirred and unstirred melts which were described in Chapter 3 as a function of bulk supercooling.

The heat transfer coefficient calculated from the interfacial temperatures of the growing crystal agree with the values predicted by the copper pot technique.

CHAPTER 6

LINEAR CRYSTALLISATION VELOCITIES IN THIN CAPILLARIES

6.1 Introduction

This study was undertaken to extend the existing range of determinations on the capillary growth rates of a benzophenone crystal made by Pickardt,[21] and also the measurements on salol made by Pollatschek[22] followed by Neumann and Micus.[23] It was then hoped to make a direct comparison of these rates with that of freely growing single crystals, in order to evaluate the usefulness of the far less labourious capillary technique of measurement as a method of obtaining surface reaction rates.

Rather unexpected results were obtained for capillary growth rates at low supercoolings. A more detailed study served to demonstrate the great importance of surface structure in determining rates of growth.

6.2 Apparatus

A series of thin pyrex glass capillaries ranging in size from about 4mm. down to 0.3mm. I.D. were employed for determining the capillary growth rates of both benzophenone and salol. These capillaries were cleaned out with chromic acid, washed thrice with distilled water and dried prior to filling with a melt, purified as already described.

6.3 Preliminary experiments on capillary growth rates of benzophenone

a) Experimental:- These runs were conducted with the undegassed benzophenone melt contained in a capillary (0.3 - 0.4mm. I.D.), sealed at one end (see figure 19). A solid plug of benzophenone was first formed at the closed end of the capillary by initiating growth at the open end of the capillary with a benzophenone crystal and permitting rapid growth down the capillary at about 20°C, i.e. 28°C supercooling. This was to ensure that the crystal was deposited with the fast growing face parallel to the capillary axis. A small narrow coal gas flame was then directed towards the capillary and the crystal melted, commencing from the open end of the capillary, to a predetermined mark leaving a plug of approximately 2cm of the crystal in the capillary, at the sealed end. The incidence of capillary fracture during the remelting process was minimised by melting the crystal down from the open end, as it allowed room for expansion arising from density differences between solid and liquid.

The capillary was then immersed in the constant temperature bath described in section 2.1, clamped in position, and each run started off from just above the above mentioned mark on the capillary wall. The displacement of the crystal surface was followed with a cathetometer, equipped with a polaroid disc within the eyepiece which served to

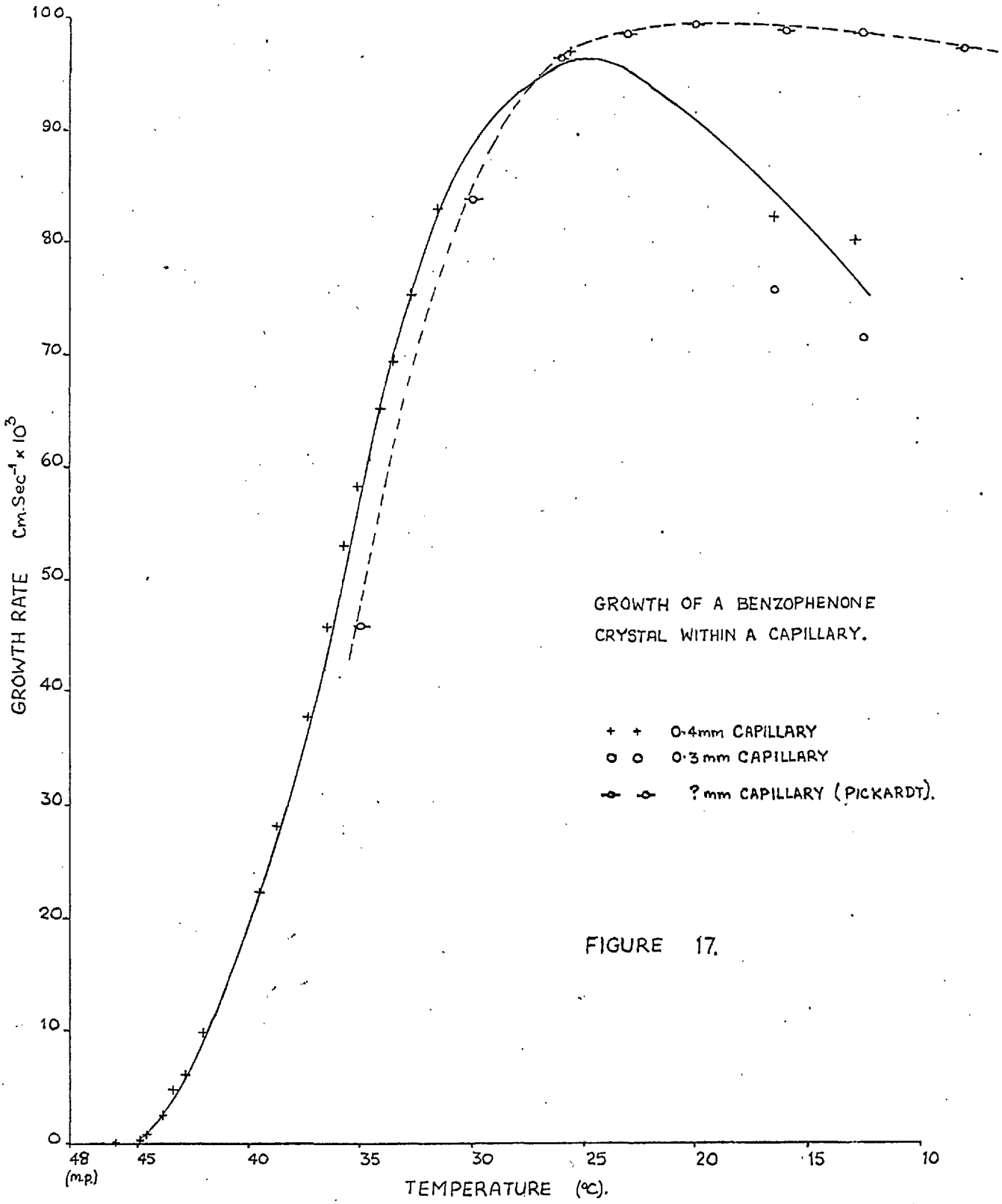
GROWTH RATE Cm.Sec^{-1} x 10^3
100
90
80
70
60
50
40
30
20
10
0
48 (m.p.)
45
40
35
30
25
20
15
10
TEMPERATURE (°C).
GROWTH OF A BENZOPHENONE CRYSTAL WITHIN A CAPILLARY.
+ + 0·4mm CAPILLARY
o o 0·3mm CAPILLARY
-o-o- ? mm CAPILLARY (PICKARDT).

FIGURE 17.

render visible the interface, which was otherwise difficult to locate. The duration of each run ranged from about 60 seconds for the highest crystallisation velocities to about 15 minutes with the slowest.

b) Results and discussion:- The capillary crystallisation velocities of a benzophenone melt are given in table 11 and illustrated by figure 17 for a number of bath temperatures ranging from 45.9°C to 14.8°C. In this range of observation (Δ T°s from 2.1°C to 33.2°C) the crystallisation velocity increased from 0.0486 x 10^{-3} cm.sec^{-1} at 2.1 deg C supercooling to a maximum of 96.7 x 10^{-3} cm.sec^{-1} at 22.5 deg C supercooling, and gradually decreased thereafter at a rate which was dependent on the diameter of the glass capillary.

The results obtained by Pickardt which are also illustrated on the same figure show good agreement as to maximum crystallisation velocity. But at supercoolings below that of the maximum the rates obtained by Pickardt are generally rather lower than those described here; and at supercoolings in excess of the maximum Pickardt observed a fairly uniform rate independent of supercooling, in contrast to a marked fall in rate observed in our own experiments. This difference in behaviour is very similar to that between the findings of Pollatschek and those of Neumann and Micus on the capillary growth of salol. Now Neumann

and Micus employed capillaries of 0.4mm diameter whereas Pollatschek used 7mm diameter tubes: and it was thought that the difference in the benzophenone results may be due to a similar difference in the diameters of the tubes employed. Whether this is really so remains a matter for surmise, as Pickardt makes no mention in his paper of the cross sectional diameters of the tubes he employed.

A most unexpected finding of this experiment was that the capillary growth rates (which were probably those of the fastest growing (001) face), were much smaller than the free growth rates of the (001) face at supercoolings of $< 4^{\circ}C$; viz. at 2.1 deg C supercooling, a capillary growth rate of 0.0486×10^{-3} cm.sec^{-1} compares with free growth rates of 0.21×10^{-3} and 0.54×10^{-3} cm.sec^{-1} from unstirred and stirred melts respectively. With bulk supercoolings in excess of 4 deg C, however, the reverse is true; in a melt supercooled 6 deg C the capillary growth rate was 9.82×10^{-3} cm.sec^{-1}, while the free growing rates from the unstirred and stirred melts were 1.35×10^{-3} and 3.42×10^{-3} cm.sec^{-1} respectively.

6.4 Preliminary experiments on capillary growth rates of salol

a) Experimental:- The experimental procedure adopted was similar to that employed with benzophenone, described in section 6.3, except

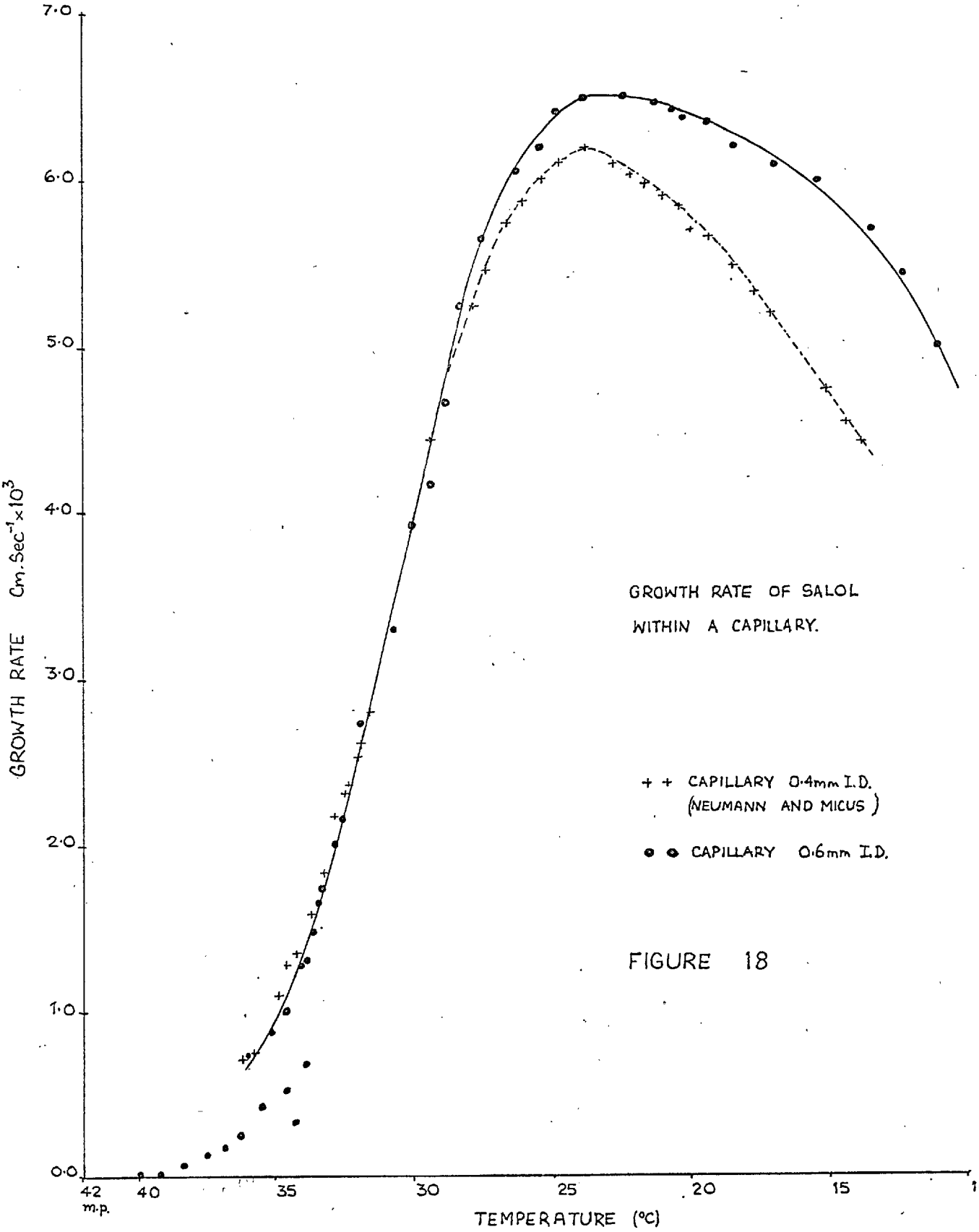
7·0
6·0
5·0
4·0
3·0
2·0
1·0
0·0
GROWTH RATE Cm. Sec^{-1} × 10^{3}
42
m.p.
40
35
30
25
20
15
10
TEMPERATURE (°C)
GROWTH RATE OF SALOL
WITHIN A CAPILLARY.
+ + CAPILLARY 0·4mm I.D.
(NEUMANN AND MICUS)
o o CAPILLARY 0·6mm I.D.

FIGURE 18

for the following modifications:

A 0.6mm I.D. capillary was filled with the purified salol and degassed in situ by three repeated cycles of solidification followed by remelting under a vacuum of about 10^{-2}mm mercury provided by an Edwards High Vacuum pump. The open end of the capillary was then attached to a water pump and maintained under this vacuum while rate measurements were being made.

The duration of each run varied from 10 minutes to about 45 minutes.

b) Results and discussion:- The results of these experiments are tabulated in table 12 and illustrated by figure 18. A fall in growth rate is observed on increasing the supercooling beyond 19.6 deg C, but these rates were higher than those observed by Neumann and Micus, though less than those reported by Pollatschek. These differences can probably be ascribed to the differences in capillary diameters, as mentioned in section 6.3.

This fall in growth rate at high supercoolings observed in fine capillaries appears to be connected with the nature of the solid phase deposited. At these large supercoolings the crystal grows along the capillary as an opaque polycrystalline front rather than as

a single crystal. There appears to be some considerable variation in the rate of growth of each crystallite, with some regions on the crystal front growing faster than others; the net result being a continuous change in the shape of the crystal front and a discontinuously variable rate of advancement along the capillary. The larger the diameter of the capillary the greater the chance of the presence of a rapid growing crystallite, and consequently the observed rates in the larger tubes are higher than those in the finer capillaries.

At supercoolings below that of the maximum crystallising velocity, the results were in close agreement with those reported in the literature (see figure 18).

Rate measurements made at supercoolings below that recorded previously produced some interesting observations both in the nature of the crystal front advancing along the capillary and on the resulting rate of growth. At a temperature above 37°C, i.e. with supercoolings of less than 5 deg C, the growth within the capillary advances as a single crystal front. Below 34°C ($\Delta T > 8$ deg C), the crystal grows primarily along the capillary walls with a hollow centre which only subsequently fills in with solid; the leading crystal front has a serrated edge and is polycrystalline in appearance. Between 34 and 37°C, either form of growth is possible, the deciding factor being

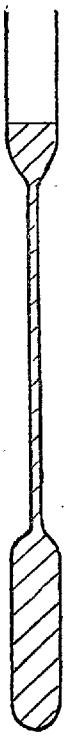

FIGURE 19

CAPILLARY USED IN THE PRELIMINARY EXPERIMENTS.

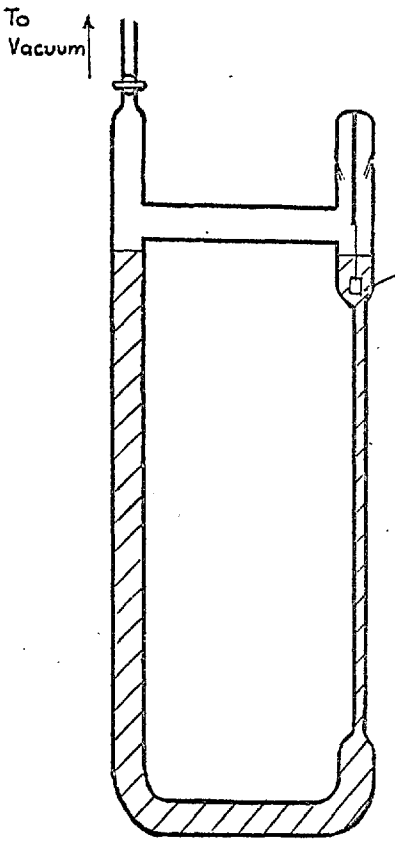

FIGURE 20.

CAPILLARY USED FOR THE DETERMINATION OF THE GROWTH RATES OF INDIVIDUAL CRYSTAL FACES.

the initial nature of the crystal front. The rate of growth of this polycrystalline front being approximately twice that of the other.

If these capillary growth rates (which probably correspond to that of the fast growing (100) face) are compared with the free growing rates of the same face (see table 4), it will be seen that the capillary rates are the smaller of the two at low supercoolings; viz. at 37.8°C i.e. 4.2 deg C supercooling, the capillary growth rate was 0.15×10^{-3} cm.sec^{-1}, while the free growing rate from the unstirred melt was approximately 0.42×10^{-3} cm.sec^{-1}.

6.5 Capillary growth rate of the slow growing (010) salol face

a) Introduction:- In the capillary growth runs so far described there was no information as to the identity of the advancing face of the crystal. Consequently, at this stage the following experiment was carried out;

b) Experimental:- A crystal of salol mounted and treated as described in section 3.5, was lowered into the melt in the widened end of the capillary (illustrated by figure 20), so that its (010) face was directly opposite the capillary mouth. The crystal was then allowed to grow into the capillary (1.5mm I.D.) at a bulk supercooling of 4.35 deg C.

c) Results:- After a short period of growth within the capillary the growth rate was 0.43×10^{-5} cm.sec^{-1} at 37.65°C ($\Delta T = 4.35$ deg C), compared with 15×10^{-5} and 50×10^{-5} cm.sec^{-1} for its free growth rate from unstirred and stirred melts respectively, at the same supercooling.

The growth rate is at least 30 times smaller in the capillary than in the bulk melt.

d) Experimental modifications:- Attempts were made also to grow the (010) salol face into the side arm of a capillary T-piece by growing the (100) face down its main limb past the junction of the capillaries. It was then found that the (010) face showed very little tendency to grow into the side limb at low supercoolings, and on further increase of supercooling a fast growing face, (which was probably the (100) face) was seen to grow along this side arm. These experiments were not pursued further.

6.6 Capillary growth rates of the fast growing (100) salol face, at low supercoolings

a) Introduction:- In view of the unexpected nature of the above result further work was undertaken along the same lines.

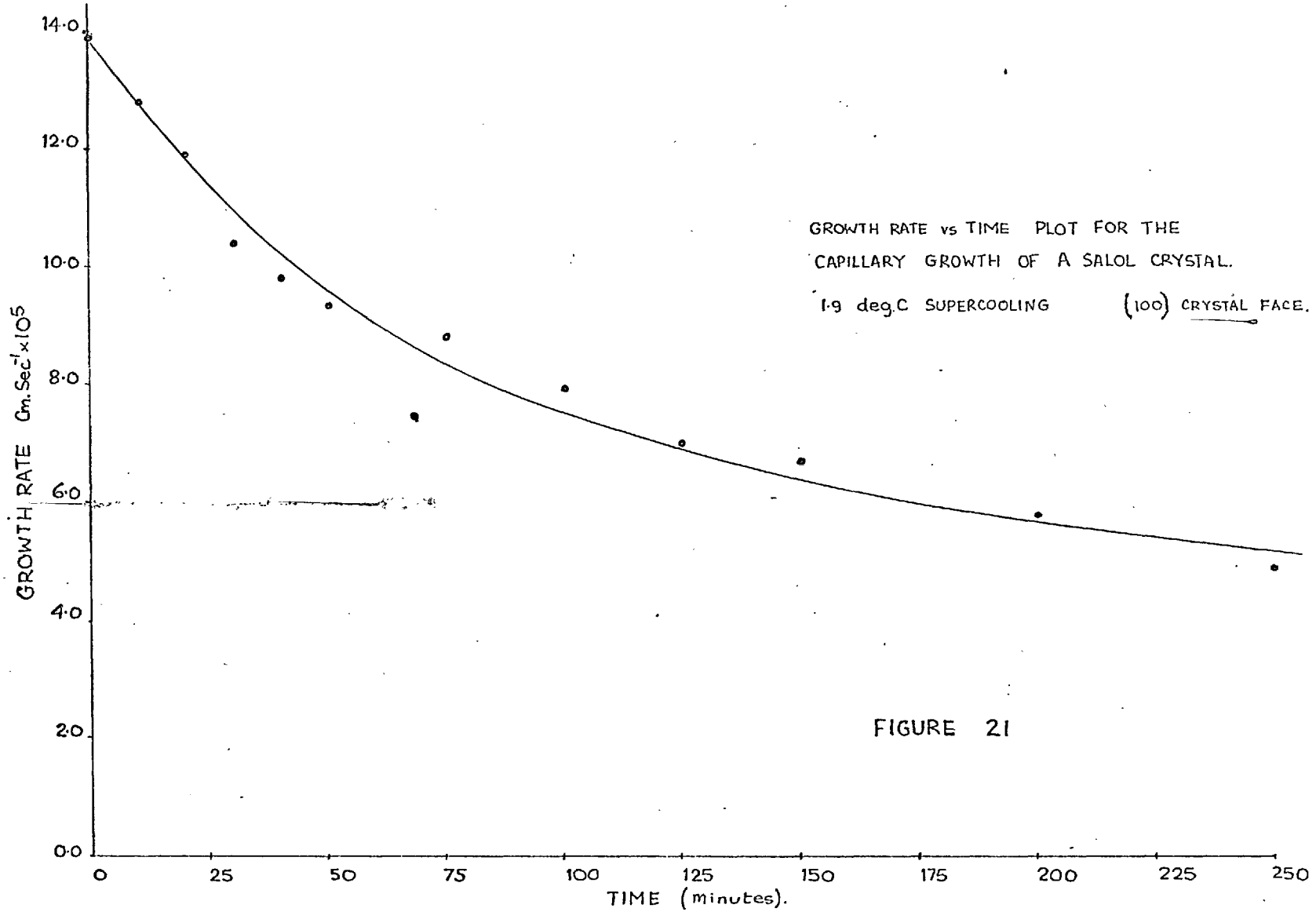

GROWTH RATE vs TIME PLOT FOR THE CAPILLARY GROWTH OF A SALOL CRYSTAL.

1·9 deg.C SUPERCOOLING (100) CRYSTAL FACE.

FIGURE 21

b) Experimental:- A crystal of salol, mounted and treated as in section 6.5, was lowered into the melt at the widened end of the capillary so that its fast growing (100) face was directly opposite the capillary (see figure 20). This was to ensure that the (100) face would subsequently grow down the capillary axis.

The duration of each run was lengthened to periods ranging from 4 hours to 4 days, and the experiments were conducted with both undegassed and degassed melts.

c) Results and discussion:- Once the crystal had grown into the capillary, its rate of advance was found to decrease with time. This is illustrated by figure 21 (table 13) in which the rate of growth of the (100) face, at a bulk supercooling of 1.9 deg C, is expressed as a function of the time of observation. These rates were obtained by drawing tangents to its displacement time curve.

The crystal grows within the capillary as a single crystal and after a period of about 4 hours growth, the rate is seen to fall to about a third of its initial value of 13.9×10^{-5} cm.sec^{-1}. Remelting a part of the newly deposited crystal material within the capillary produced initially an increase in the growth rate, which subsequently fell as before (not shown in table). Under comparable conditions of

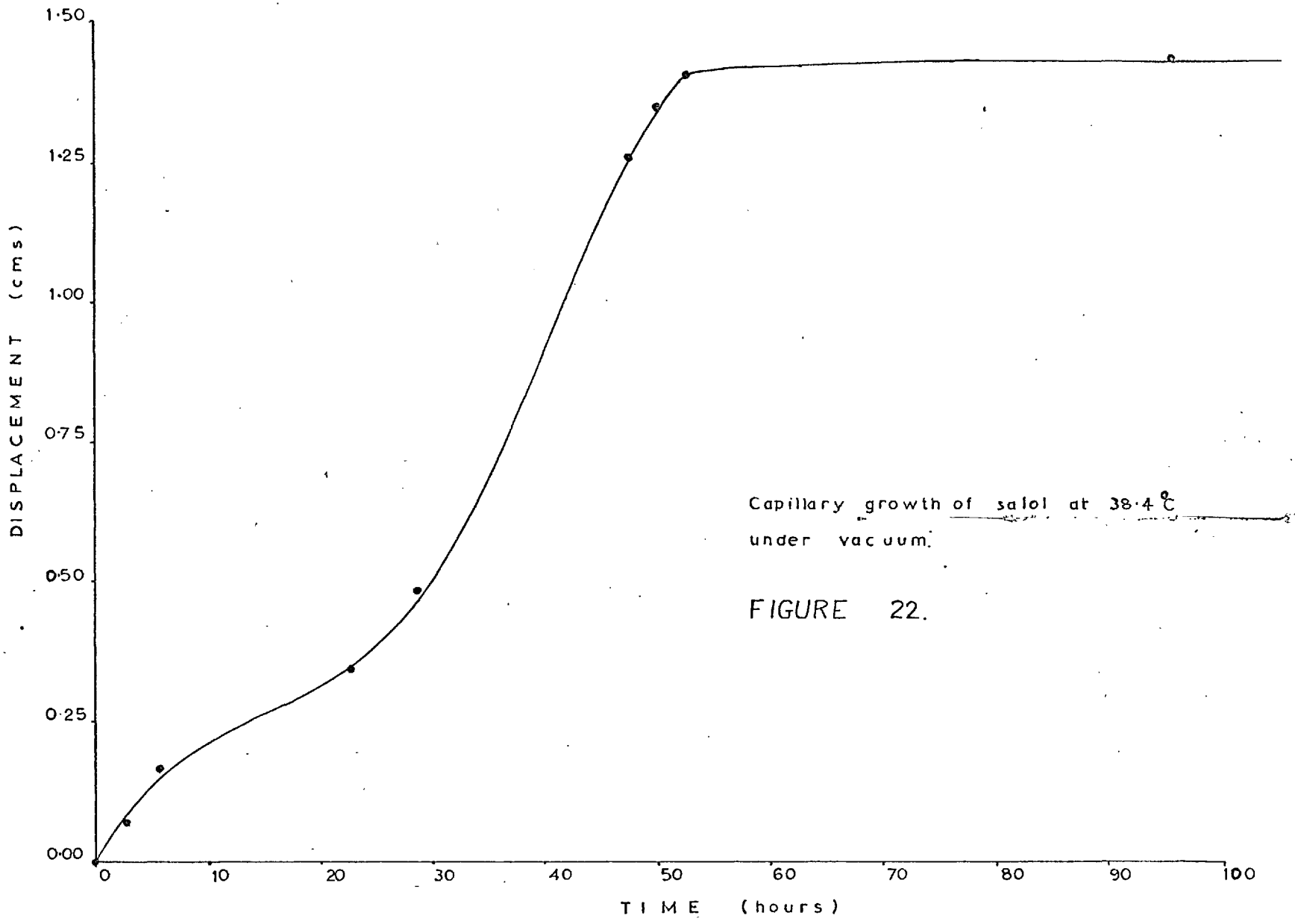

Capillary growth of salol at 38·4°C under vacuum.

FIGURE 22.

bulk supercooling the free unstirred growth rate of the (100) salol face is about 14×10^{-5} cm.sec^{-1}.

A modified experiment using a degassed melt produced the same retardation observed previously with the undegassed melt. Figure 22, (table 14) is a displacement-time plot for such a run, supercooled 3.6 deg C, wherein after 52 hours growth, the average rate for the 43 hours following was found to be over 1000 times smaller than the free (unstirred) growth rate of about 26.5 cm.sec^{-1} for the (100) face, under comparable conditions, of bulk supercooling.

Discussion of the significance of the results of all the experiments described in this chapter will be reserved till Chapter 7 section 3.

6.7 Capillary growth of benzophenone at low supercoolings

a) Introduction:- Experiments were then undertaken on benzophenone to see if this phenomenon was observed with substances other than salol.

b) Experimental:- These experiments were conducted in a 0.6mm capillary using benzophenone purified by distillation, but undegassed and under atmospheric pressure. The periods of observation ranged from 1 to 4 hours and measurements refer to the (001) face of the crystal.

GROWTH RATE vs TIME FOR THE CAPILLARY GROWTH OF BENZOPHENONE CRYSTALS. (001) FACE.

FIGURE 23

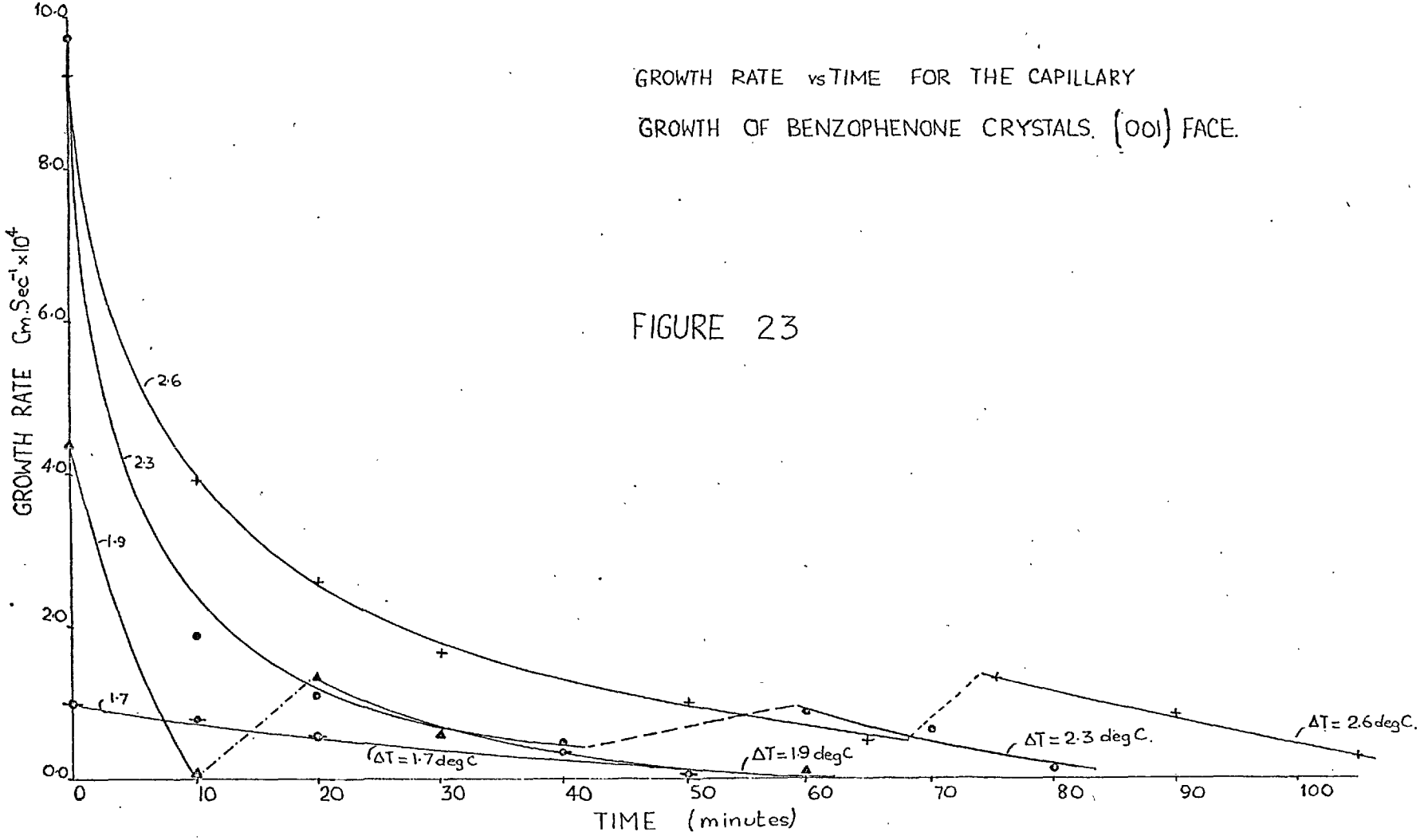

c) Results and discussion:- No appreciable retardation of growth was observed above a supercooling of 4 deg C, when growth within the capillary did not correspond to a single crystal, but was opaque in appearance and had a jagged surface for the leading edge of the crystal (see figure 23, table 15).

At lower supercoolings, however, the crystal advanced along the capillary axis as a single crystal front and the retardation was clearly observed, as illustrated by the run at 1.7 deg C bulk supercooling. In this run the rate fell continuously to a twentieth of the initial rate of 1.0×10^{-4} cm.sec^{-1} in a period of 50 minutes. At slightly higher supercoolings (but below 4 deg C, ΔT) the general tendency is for a fall in the growth rate, but instead of a continuous fall in rate there are some discontinuities in the rate plot (figure 23). These correspond to periods of more active growth.

6.8 Trace impurity effects on capillary growth

a) Introduction:- One explanation which seemed likely on the basis of several observations reported in the literature, was that the growth retardation was due to impurities which accumulate in advance of the growing face. In order to determine whether this was really so two types of experiments were conducted. In the first the

impurities were either frozen solid or bodily moved away from the growing interface and a study made on the impurity freed melt. The alternative method was an irrigation technique which employed forced circulation within the capillary, just ahead of the growing crystal. By this means it was hoped to avoid an undue build-up of the impurity concentration level and to maintain the composition of the melt as close as possible to that in the rate determining runs on the growth of free single crystals.

b) Experimental and results:- A crystal of salol was grown down a capillary of I.D. 1mm., from a melt supercooled 4.5 deg C, purified by repeated recrystallisation from ethyl alcohol. Once the crystal ceases to grow the capillary was withdrawn from the bath and the balance of the melt solidified by a large increase of supercooling. Any impurity which may have accumulated ahead of the growing interface is frozen into a region which is clearly demarcated from the rest of the crystal by a change in crystal appearance; the region corresponding to slow growth while immersed in the bath was clear and transparent, whilst the region where growth was rapid and which must have contained any impurity present, was opaque. The transparent crystal material was then melted to within about 5mm of this interface, with the solid plug serving to prevent back diffusion of any impurity present.

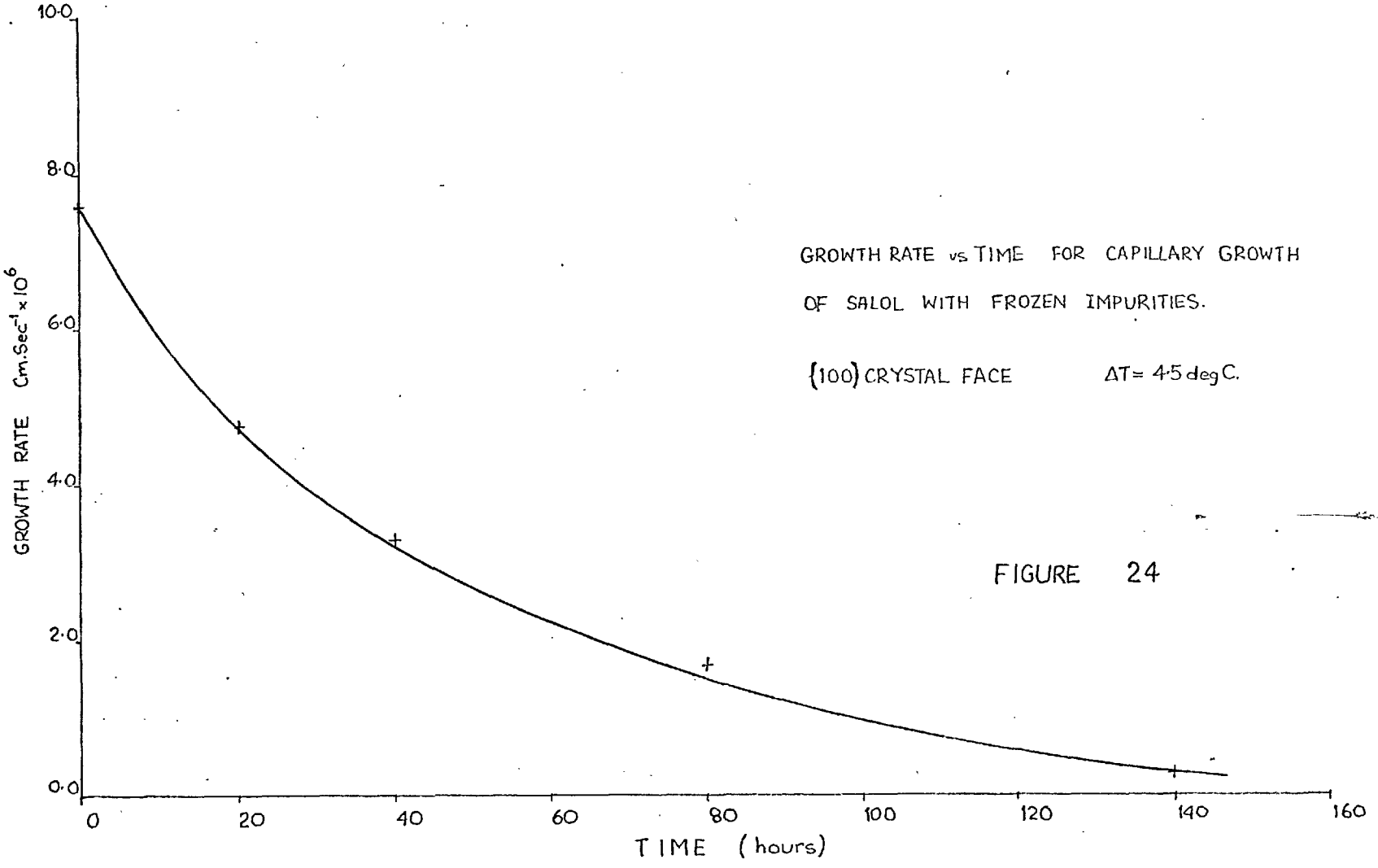

GROWTH RATE vs TIME FOR CAPILLARY GROWTH OF SALOL WITH FROZEN IMPURITIES.

{100} CRYSTAL FACE $\Delta T = 4{\cdot}5$ deg C.

FIGURE 24

GROWTH RATE vs TIME FOR CAPILLARY GROWTH OF SALOL, PURIFIED BY REPEATED RECRYSTALLISATION.

(100) CRYSTAL FACE $\Delta T = 4.5$ deg C

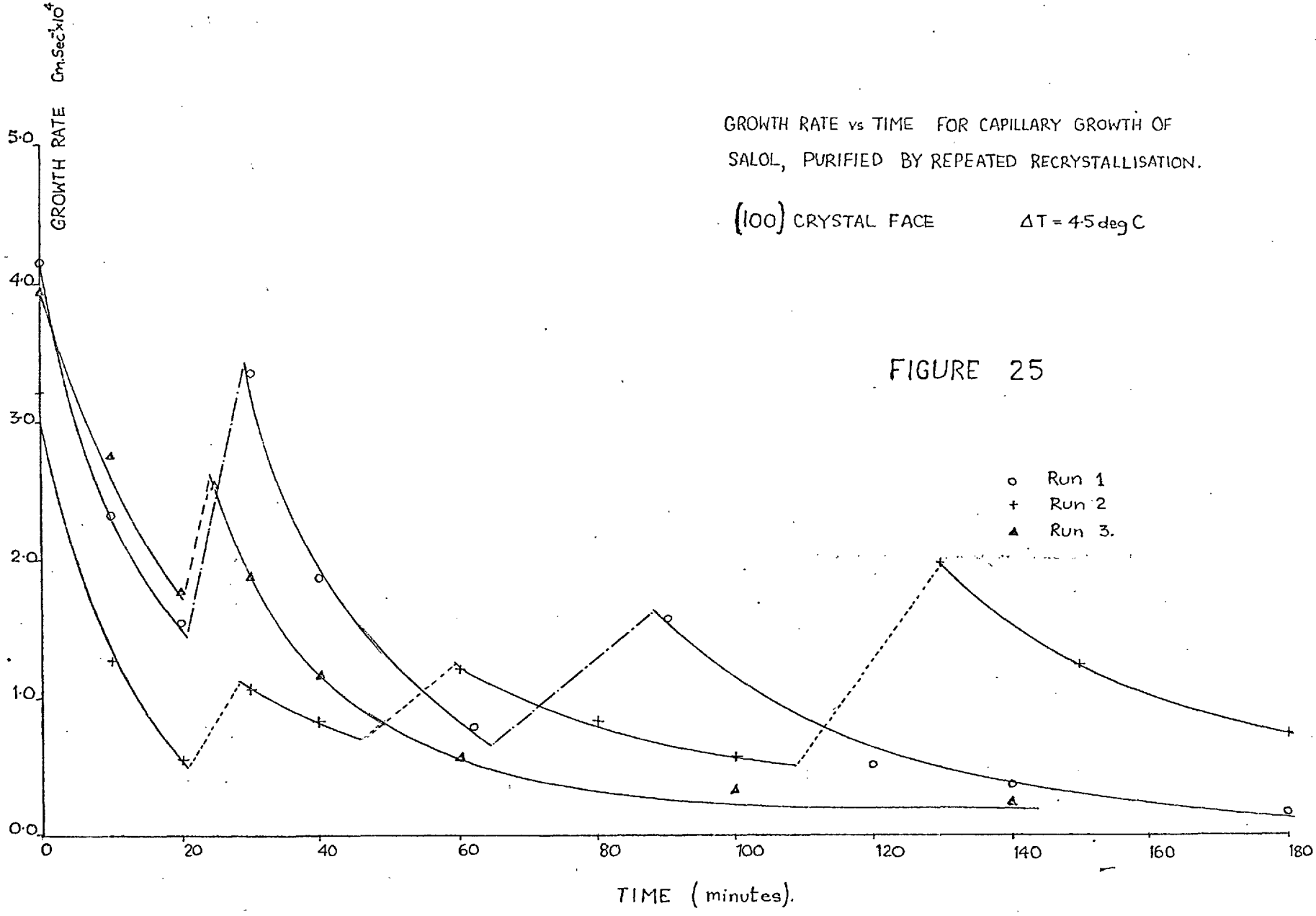

FIGURE 25

Starting from this point a reverse growth run was made through the purified column of melt.

Figure 24 (table 16), illustrates a run conducted with the capillary immersed in a bath at 37.5°C (ΔT = 4.5 deg C). Once again a continuous decrease of growth-rate is observed:

In the next series of experiments the melt was purified by a process of zone-refining within the capillary itself. This was effected by repeated cycles of growth followed by melting back to a predetermined mark on the capillary, wherefrom all rate measurements were made.

Figure 25 (table 17) illustrates that there was in general no tendency for the rates of crystallisation to increase as the melt becomes purer by successive recrystallisation. This was to be expected if contaminents were the cause of the observed retardation of rates.

The irrigation technique consisted of applying intermittent pressure on a diaphram attached to a fine capillary situated in the liquid phase within the main capillary, in order to force the melt past the growing crystal surface and avoid the concentration of any impurity present at the interface. This method too failed to yield

GROWTH RATE vs TIME FOR CAPILLARY GROWTH
OF A SALOL CRYSTAL WITH FORCED CIRCULATION.

(100) CRYSTAL FACE $\Delta T = 3.8$ deg C.

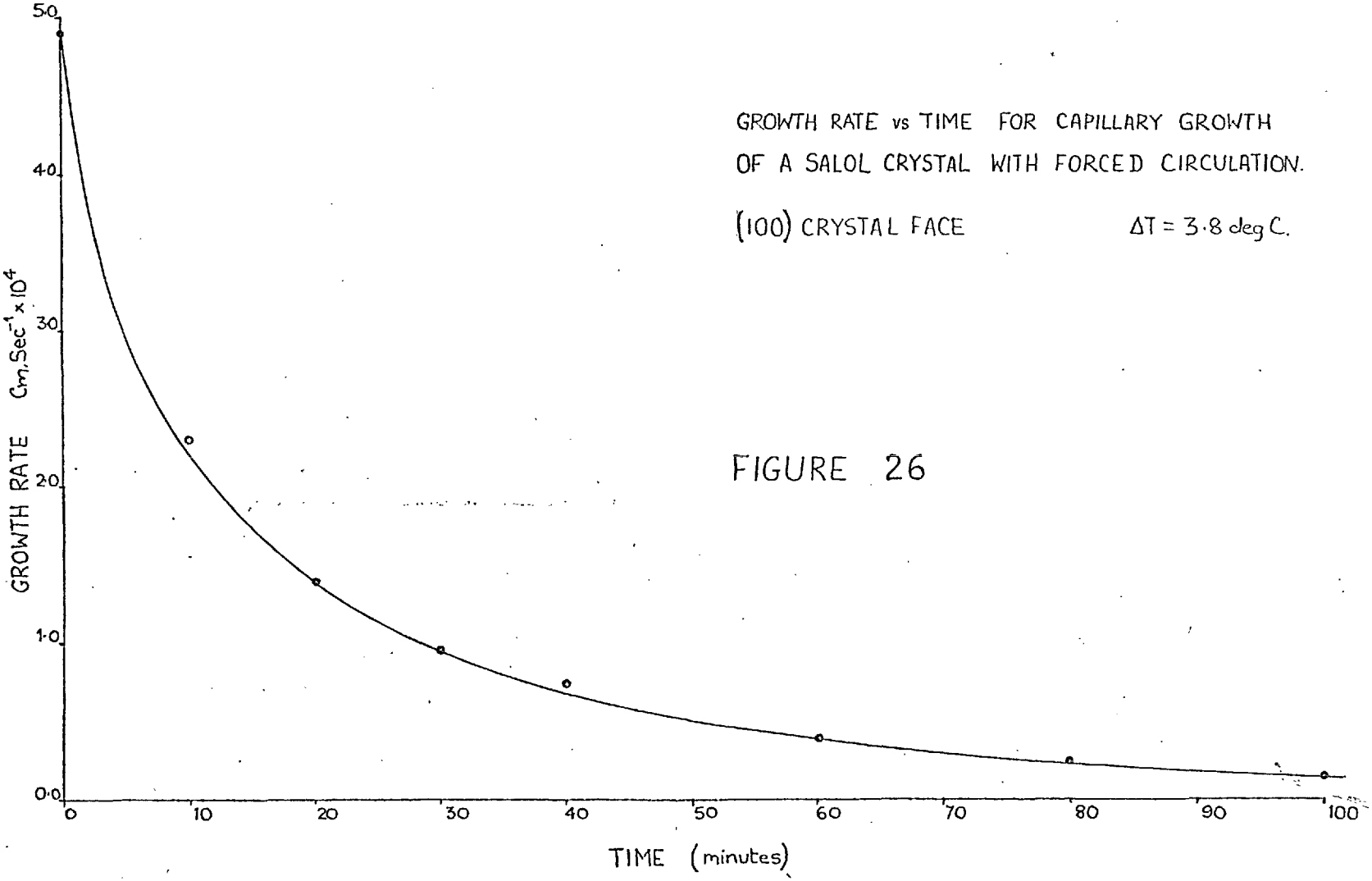

FIGURE 26

a uniform rate of growth, as illustrated by figure 26 (table 18).

b) Discussion:- None of these methods of showing up impurities as the possible cause for the retardation of growth within a fine capillary, succeeded in producing a constant rate of interfacial displacement at low supercoolings or even produced an effect different from that observed with ordinary recrystallised salol. It therefore seemed most likely that impurities could not have caused this retardation.

A point of interest is that the initial rate of growth commencing from a seed crystal which had itself been deposited by a process of slow growth within the capillary, was considerably lower than one in which the seed had been deposited more rapidly. Thus an initial rate from a slowly deposited crystal of 0.0755×10^{-4} cm.sec^{-1} (see figure 24), compares with about 3×10^{-4} cm.sec^{-1} at the same supercooling of 4.5 deg C in figure 25 and 4.9×10^{-4} cm.sec^{-1} in figure 26 at a bulk supercooling of only 3.8 deg C.

6.9 Surface structure sensitivity of capillary growth rates

a) Experimental:- All these observations on the retardation of growth in capillaries suggested that growth might be a function of the perfection of the crystal surface. For instance dislocations

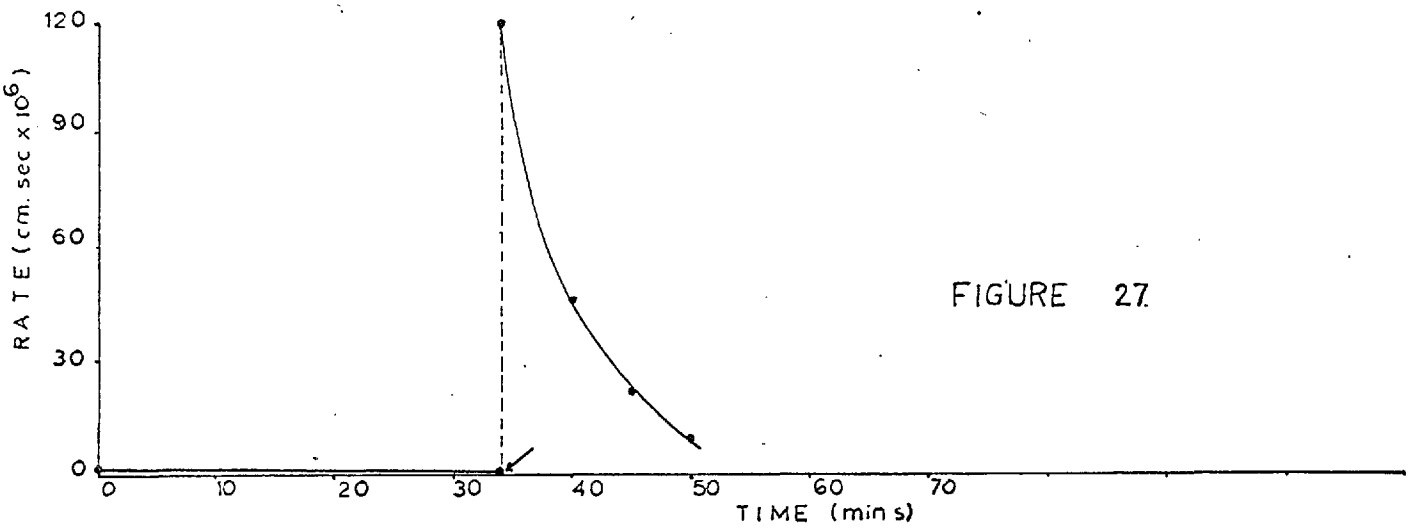

FIGURE 27.

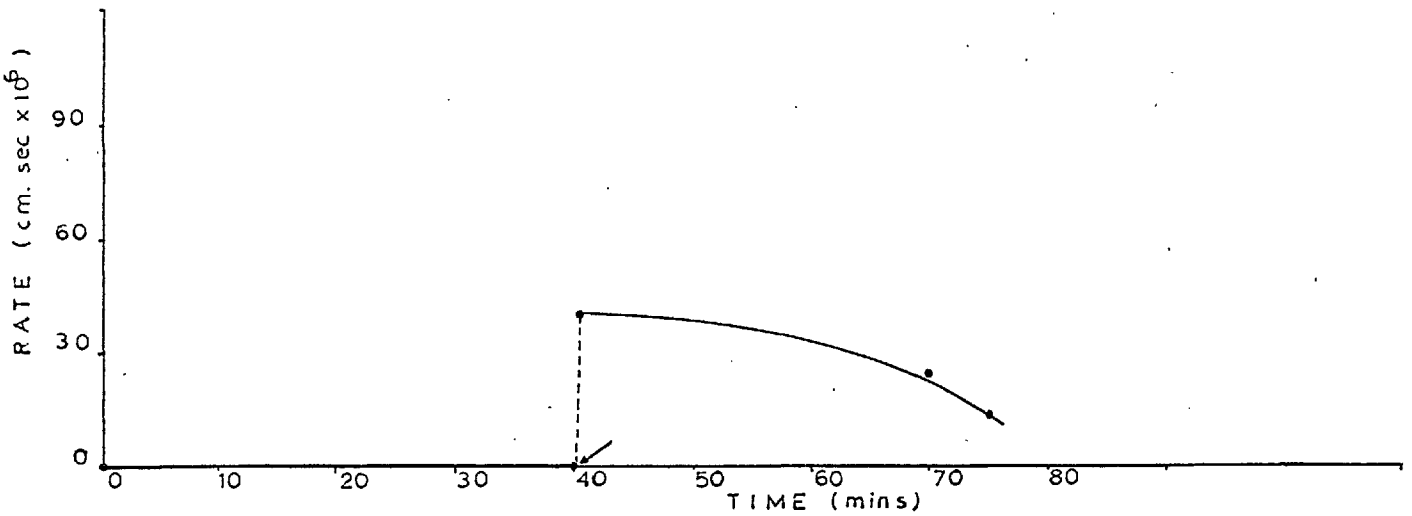

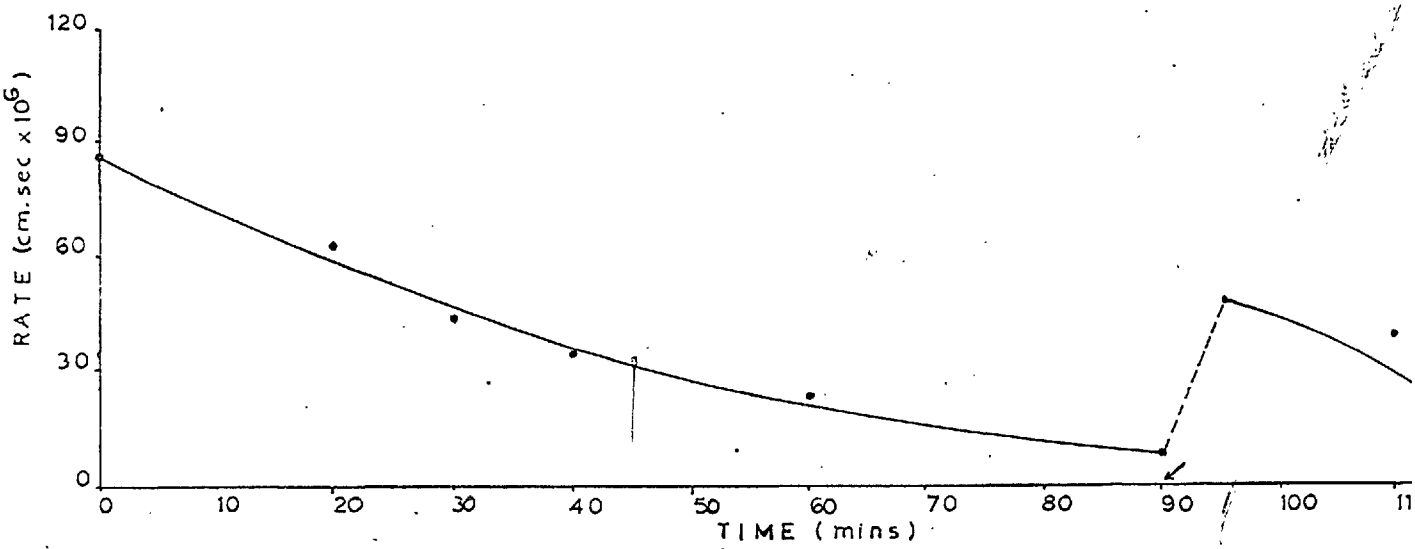

Capillary growth of benzophenone at 2°C supercooling.

↓ Denotes time of surface disturbance

initially present might grow out to the walls of the capillary and leave a more perfect surface. This idea led to experiments in which imperfections were artificially induced on the crystal surface within the capillary. Experimentally this consisted of touching the surface of a crystal which had practically ceased to grow with a fine glass spike. The capillary employed had an internal diameter of 1.5mm and the diameter of the spike was approximately 0.6mm. The surface under observation was that of the (001) face of the benzophenone crystal.

b) Results and discussion:- A large increase of growth rate is observed when the crystal surface is touched with a glass rod, but thereafter the rate falls progressively back again in the usual way to the low rate from which it started. The figures are given in table 19 and are illustrated in figure 27.

These observations are consistent with the view that growth-rates in capillaries are surface structure sensitive and that the observed fall in rate is probably due to the growing out of surface defects.

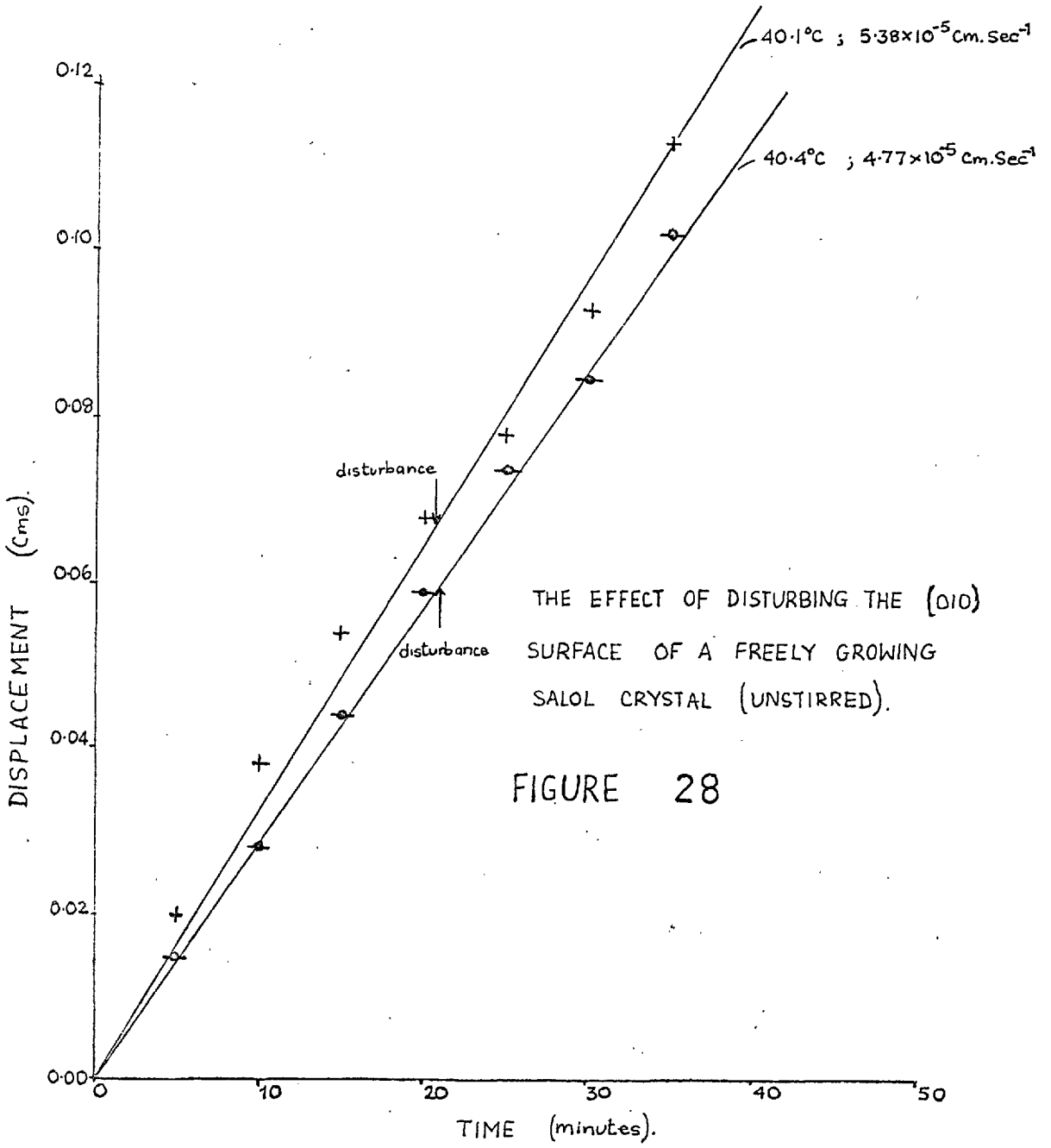

THE EFFECT OF DISTURBING THE (010) SURFACE OF A FREELY GROWING SALOL CRYSTAL (UNSTIRRED).

FIGURE 28

6.10 The effect of a surface disturbance on the free growth rate of the (010) face of a salol crystal

a) Introduction:- Surface defects were artificially induced on the surface of a freely growing crystal in order to determine whether an effect similar to that observed in capillaries was present in the growth of free single crystals.

b) Experimental:- The (010) surface of a crystal of salol growing freely from a melt in the manner described in section 3.5 was touched with a glass spike. The bulk supercooling of the melt was kept below 2 deg C and the crystal was touched after an initial period of growth of about 1 hour.

c) Results and discussion:- No observable change of growth rate is registered on touching the crystal. This is indicated by figure 28 (table 20). As discussed later a likely explanation for the difference in behaviour is that the surface structure of a freely growing crystal under these conditions of supercooling is far from ideal and has already a sufficient concentration of surface imperfections for the added deformation to have no further influence on the rate of growth.

6.11 Summary

At low supercoolings the capillary growth rates of both benzophenone and salol were found to be surprisingly lower than that of their respective free growth rates, under comparable conditions. A more detailed examination shows that the capillary rates of growth at very low supercoolings fall over a considerable period of time after entry into the capillary, until growth is almost completely arrested. Further purification of the melt does not help to yield a uniform rate capillary growth, thus eliminating impurities as a possible cause for growth retardation. These rates are then shown to be sensitive to mechanical surface disturbance in contrast to the growth of free single crystals which do not exhibit this sensitivity under the experimental conditions.

CHAPTER 7

DISCUSSION

7.1 Nucleation

In this investigation the mechanism of breeding has been studied in supercooled benzophenone melts under unstirred conditions; it is believed that this is the first investigation of breeding in supercooled melts.

The tendency to breed on the introduction of a crystal into a supercooled melt, which is quite small at low supercoolings, increases rapidly in melts whose supercooling exceeds about 9 deg C. These newly formed crystals which take the form of needle-like growths originate at the surface of the seed crystal, grow for a short period, and then detach themselves from the seed, probably on account of their weight. Only one crop of needle-like growths are observed on the surface of the seed, and these newly formed crystals do not appear to be capable of further breeding except by a collision process which will be discussed later.

Examination under the polarising microscope showed that these needle-like growths have different extinction angles from that of the parent crystal and from one another, from which it would follow that they do not constitute a part of the lattice of the parent crystal; this would also explain the ease of their detachment.

The view that these needle-like growths originate from active dusts on the surface of the parent crystal is confirmed by the finding that a crystal grown for an initial period at a very low supercooling would subsequently grow as a single crystal on re-immersion in a highly supercooled melt without showing any tendency to breed.

These dusts, which are probably microcrystalline particles of benzophenone, may have been produced while the parent crystals were being dislodged from the rod on which they were initially produced or in the subsequent process of storage or even during the process of mounting on the glass spike.

Mason[4] has made a detailed study of the mechanism of breeding in supersaturated aqueous solutions of magnesium sulphate heptahydrate. He concluded that breeding in this system could be due to the presence of microcrystalline particles on the surface of the parent crystal which produce an initial crop of new nuclei, as observed by us with benzophenone. Mason also observed several other processes by which breeding can continue beyond the initial crop: these processes were not observed in the case of benzophenone.

All the discussion on breeding given above refers to isolated crystals growing out of contact with other solids. It was observed

by us in the case of benzophenone that when the fast growing (001) face makes contact with the walls of the vessel several crystals are observed to grow outwards in all directions from this point of contact. This phenomenon is very similar to the collision breeding observed by Mason, in which breeding occurs due to collisions between the crystals themselves or between the crystal and the walls of the containing vessel.

7.2 'Free' growth rates

Once the mechanism of breeding in supercooled melts was understood (and subsequently eliminated by the use of 'surface healed' seeds), it became possible to grow crystals from the melts over a wide range of bulk supercoolings and study the kinetics of growth of a single crystal free from unwanted secondary nucleation.

Measurements showed that the rates of growth of the fast growing (001) benzophenone face from the melt increased more than linearly with increase of supercooling in both stirred and unstirred melts. The rates in stirred melts were, moreover, very considerably larger than the unstirred rates: this effect was shown not to be due to impurity build up in front of the growing face, and it was clearly due to heat transfer effects, which are applicable even in the case of such slow growing materials as benzophenone and salol.

From the very large increase of rate observed on stirring it is evident that the heat transfer control of the unstirred run must be very considerable; to quote a rather typical example, the stirred rate of growth at a bulk supercooling of 1.8 deg C is 46.2×10^{-5} cm.sec^{-1} while the corresponding unstirred rate was 17.6×10^{-5} cm.sec^{-1}.

It can be argued that if rates were substantially heat transfer controlled, then it is to be expected that growth rates should increase with increase of bulk supercooling in a manner similar to that of the anticipated change in the rate of heat transfer. It is, however, found experimentally that the observed unstirred rates of growth would require the heat transfer coefficient to increase with supercooling as $\Delta T^{0.8}$, while the actual rate of increase of this coefficient due to natural convection is usually taken to be only as $\Delta T^{0.25}$.

A similar difference in rate between stirred and unstirred runs was observed even on the slower growing (010) salol face; for instance, at a bulk supercooling of 1.6 deg C the stirred rate was almost 6 times that of the unstirred rate of 1.19×10^{-5} cm.sec^{-1}, showing the importance of heat transfer even at these very low growth rates.

Copper pot experiments:- In order to investigate further the above

results, it seemed to be desirable to obtain independent measurements of the heat transfer coefficient, under varying degrees of agitation in the liquid phase, and these were obtained with an electrically heated copper pot.

In unstirred melts of benzophenone this coefficient increased only slightly with interfacial temperature difference, as illustrated in figure 10, curve III. As would be expected agitation produced a marked increase in this coefficient as illustrated by curves IV - VI on the same figure. However, what seems difficult to understand is why this coefficient should, at constant Reynolds Number, initially increase so sharply with ΔT as shown on the curves: the coefficient is usually assumed to exhibit little or no dependence on ΔT in stirred fluids.

Very similar results illustrated in figure 11, have been obtained for the coefficient of heat transfer in melts of salol.

Further anomalies are encountered if the heat transfer coefficient derived by copper pot measurement are compared with the observed growth rates: for instance as shown in tables 5 and 6, figure 10 the experimentally observed unstirred growth rate of benzophenone is about 5 times as fast as the maximum rate permissible by the experimentally determined coefficient of heat transfer.

Possible explanations of this discrepancy may be enumerated as follows:-

a) The size of the copper vessel was much larger than that of the crystal; the length of a benzophenone crystal was 5 - 15mm with the (001) face never exceeding 1 - 2mm side, while one side of the copper vessel was 16mm in length. The application of dimensional analysis predicts that the coefficient of heat transfer would, for given Reynolds Number, vary inversely as a characteristic dimension of length of the surface across which heat is transferred and therefore a factor of 5 between the coefficient operative on the (001) face and that determined on the copper pot would not seem unreasonable.

b) Another point of difference between the two coefficients is an unknown factor due to inherent differences in shape and orientation. Under the experimental conditions the benzophenone crystal grew downwards with the leading (001) face flat and horizontal while a large proportion of the heat transfer surface on the copper vessel was curved and vertical.

Thermocouple experiments:- These difficulties of interpretation of the results of the copper pot experiments led to a further method of investigation in which thermocouples were used to determine surface

temperatures: the results of these experiments were considered to be far more meaningful than those of the copper pot technique. From the non-uniformity of the surface temperatures observed in the experiments it became evident that a part of the heat generated on a fast growing face could be conducted through the crystal and dissipated into the melt through a slow growing and consequently cooler face. Such a mechanism would provide yet another explanation as to how the observed rate of growth could exceed that imposed by heat transfer limitations based on a coefficient of heat transfer obtained with the copper pot.

Furthermore the thermocouple measurements showed beyond doubt that the unstirred rates were substantially heat transfer controlled.

The introduction of thermocouples into the system did not appear to have an appreciable effect on growth rates, and the heat transfer coefficient calculated from the surface temperatures of the slow growing (010) face of a salol crystal determined with thermocouples, agreed with that measured on the copper pot. This agreement tends to confirm the validity of both methods of measurement.

However far the most important result of the thermocouple experiments was the production of the unique growth curve (figure 13) in which presumably heat transfer effects were wholly eliminated.

This in turn led to a statistical analysis of the results, which showed that the rates of growth of the (010) face of salol could be expressed by the empirical result $R_n = 3.6 \times 10^{-5} (\Delta T_i)^{2.0} cm.sec^{-1}$.

Experimental data currently available on crystallising velocities from the melt have mostly been determined in capillaries. The introduction of a capillary has been shown in the present work to reduce the growth rate enormously as compared with the bulk growth rate at low supercoolings and it is therefore suggested that the expression given above for the growth kinetics of the (010) salol face is likely to be one of the few that are valid for the free growth of a crystal outside of a capillary.

Hillig and Turnbull[24] have derived a theoretical equation for the growth of a crystal from the melt by a screw dislocation mechanism. According to this equation the rate is proportional to ΔT^2. This is clearly in complete agreement with the experimentally observed result for the (010) salol face, quoted above.

7.3 Growth rates within fine capillaries

The rates of growth in fine capillaries are generally considered to approximate surface reaction rates on the assumption that heat could be conducted away more easily from the growing surface in a

fine capillary than from the plane surface of a free growing crystal. Hence it was thought desirable to obtain by this means, confirmation of the surface reaction rates determined by the thermocouple technique.

a) High supercoolings:- At supercoolings below that of the maximum crystallising velocity but in excess of 4 deg C, the capillary rates of growth illustrated in figure 17 were in fair agreement with those of Pickardt[21]. On further increase of supercooling a fall in rate is now observed whereas Pickardt reported a fairly uniform rate. This difference is attributed to possible differences in the diameters of the capillaries in which measurements were made. It has been generally observed that at high supercoolings rates decrease with decreasing diameter. This last relationship which is contrary to expectation from considerations of heat transfer can be explained on the basis that growth under these conditions of large supercooling is polycrystalline: that is to say the solid phase is polycrystalline, and the front advances by the nucleation of a succession of micro-crystals at the front (this is visually obvious). The rate of advance of the front will be subject to very complex laws, but may well depend on diameter in the way suggested above.

A similar result has been previously reported by Neumann and Micus[23] by comparing their results on the capillary growth rates of

salol with that of the earlier work by Pollatschek[22]. These observations by Neumann and Micus have also been confirmed in this present study.

b) Low supercoolings:- Under conditions of low bulk supercoolings it is found that the capillary rate was far smaller than the bulk rate. Furthermore if a bulk crystal was allowed to grow into a capillary it was found that the rate of growth kept on decreasing with time of observation until eventually growth was almost completely arrested.

In explanation of these observations appeal may be made to the theories of Frank[25], who postulates that the rate of growth of crystals is frequently determined by the presence of screw dislocations, and that a dislocation free crystal would only grow extremely slowly. These dislocations are self-perpetuating, and provide continuing growth centres in the face of a growing crystal.

It would therefore be easy to understand that any dislocation initially present in a crystal growing in a fine capillary might grow out towards the wall and cease to exist. Provided at the same time it is assumed that fresh dislocations are not created, the growing surface would soon become dislocation free, and according to Frank, cease to grow.

Such a hypothesis receives considerable support from the observation that the mechanical introduction of a gross surface deformity on a crystal surface had the immediate effect of reactivating the growth process in a crystal which had previously ceased to grow within a capillary.

It is believed that this very strong decrease of growth rate within a capillary at low supercoolings has not been reported before. However, this phenomenon is probably related to the observation that has frequently been made to the effect that gross distortions of crystals appear to have very marked effects on growth rates: to quote one example only Hillig[11] has observed that imperfect crystals of ice grow from supercooled water about 300 times faster than perfect ones, at 0.03 deg C supercooling.

APPENDIX I

Table 1: (Figure 4) Experimental Results

Growth of the (001) benzophenone crystal face from supercooled melts

T°C	△ T°C	Unstirred growth-rate $cm.sec^{-1} \times 10^5$	Stirred growth-rates $cm.sec^{-1} \times 10^5$
39.3	8.7	745	-
40.2	7.8	400	-
41.0	7.0	203	-
41.0	7.0	211	-
41.1	6.9	340	680
42.0	6.0	135	342
42.3	5.7	166	-
43.0	5.0	97.1	247
43.2	4.8	86.0	-
43.2	4.8	83.0	-
44.0	4.0	66.7	133
44.7	3.3	41.0	-
44.7	3.3	44.4	-
45.0	3.0	30.5	87.8
45.7	2.3	24.4	-
46.2	1.9	17.6	46.2
46.2	1.8	13.6	41.2
46.6	1.4	14.1	-
47.0	1.0	7.75	31.7
47.0	1.0	8.78	-
47.2	0.8	9.94	-
47.5	0.5	6.67	-

Table 2: (Figure 4)

Growth of the (001) benzophenone crystal face from a zone-refined melt.

T°C	$\triangle$ T°C	Unstirred growth-rate $cm.sec^{-1} \times 10^5$	Stirred growth-rates $cm.sec^{-1} \times 10^5$
42.4	5.6	117	193
42.4	5.6	117	-
44.6	3.4	55.6	91.0
45.9	2.1	30.3	55.6

Table 3: (Figure 6)

Growth of the (010) salol crystal face from supercooled melts

T°C	Δ T°C	Unstirred growth-rate $cm.sec^{-1} \times 10^5$	Stirred growth-rate $cm.sec^{-1} \times 10^5$
34.2	7.8	41.2	-
35.3	6.7	34.4	-
36.2	5.8	27.3	83.5
37.1	4.9	13.9	-
37.2	4.8	-	66.7
37.3	4.7	14.2	-
37.6	4.4	-	52.0
38.0	4.0	11.9	47.6
38.3	3.7	8.23	-
38.8	3.2	5.85	-
39.2	2.8	6.8	27.8
39.3	2.7	6.67	31.3
40.0	2.0	4.26	13.5
40.4	1.6	1.19	6.69

Table 4: (Figure 7)

Growth from unstirred melts of the (100) face of a phenyl salicylate crystal.

Bath temperature T°C	Supercooling Δ T°C	Growth-rate cm.sec^{-1} x 10^5
35.9	6.1	45.5
36.7	5.3	37.6
37.6	4.4	27.6
38.0	4.0	27.7
39.0	3.0	21.7
39.4	2.6	17.8
40.7	1.3	9.40
40.8	1.2	9.07

Table 5: (Figure 10)

Experimental coefficients of film heat transfer into unstirred benzophenone melts.

i (amps)	v (volts)	Q ($Cal.sec^{-1}$)	Thermocouple Δ μV	ΔT (^{o}C)	$\frac{Q}{A \Delta T} = h$ $cal.sec^{-1}cm^{-2}{}^{o}C^{-1}$
0.160	1.10	0.0419	103	2.40	.00267
0.190	1.37	0.0618	132	3.04	.00308
0.220	1.50	0.0785	165	3.86	.00312
0.250	1.70	0.101	200	4.68	.00332
0.300	2.05	0.147	263	6.14	.00362
0.340	2.30	0.186	318	7.42	.00383
0.380	2.60	0.235	376	8.78	.00409
0.420	2.85	0.283	439	10.25	.00422
0.460	3.12	0.343	505	11.8	.00444
0.500	3.42	0.407	574	13.4	.00464
0.540	3.70	0.476	642	15.0	.00485

Table 5: cont'd

Experimental coefficients of film heat transfer into stirred benzophenone melts.

Rate of stirring :- 475 r.p.m.

i (amps)	v (volts)	Q ($Cal.sec^{-1}$)	Thermocouple $\Delta \mu V$	ΔT (°C)	$\frac{Q}{A \Delta T} = h$ $cal.sec^{-1}cm^{-2}{}^{o}C^{-1}$
0.160	1.10	0.0419	28	0.65	0.00981
0.250	1.70	0.101	50	1.17	0.0133
0.350	2.40	0.201	85	1.99	0.0154
0.450	3.05	0.328	135	3.16	0.0158
0.550	3.75	0.493	194	4.54	0.0166
0.650	4.43	0.689	267	6.24	0.0169

Table 5: cont'd

Experimental coefficients of film heat transfer into stirred benzophenone melts.

Rate of stirring :- 625 r.p.m.

i (amps)	v (volts)	Q ($Cal.sec^{-1}$)	Thermocouple $\Delta\mu V$	ΔT (°C)	$\frac{Q}{A\ \Delta T} = h$ $cal.sec^{-1}cm^{-2}{}^{o}C^{-1}$
0.160	1.10	0.0419	15	0.35	0.0183
0.200	1.37	0.0630	22	0.51	0.0186
0.250	1.70	0.101	35	0.82	0.0188
0.300	2.05	0.147	49	1.14	0.0195
0.350	2.40	0.201	66	1.54	0.0198
0.400	2.70	0.258	84	1.96	0.0201
0.450	3.05	0.328	108	2.52	0.0198
0.500	3.40	0.406	131	3.06	0.0203
0.550	3.75	0.493	159	3.72	0.0203
0.600	4.10	0.587	185	4.33	0.0208

Table 5: cont'd

Experimental coefficients of film heat transfer into stirred benzophenone melts.

Rate of stirring :- 870 r.p.m.

i (amps)	v (volts)	Q ($Cal.sec^{-1}$)	Thermocouple Δ μV	ΔT (°C)	$\frac{Q}{A \Delta T} = h$ $cal.sec.^{-1}cm^{-2}{}^{o}C^{-1}$
0.160	1.10	0.0419	13	0.30	0.0212
0.250	1.70	0.101	28	0.65	0.0237
0.350	2.38	0.201	55	1.28	0.0238
0.450	3.08	0.330	88	2.05	0.0241
0.550	3.75	0.493	132	3.08	0.0244
0.650	4.45	0.671	185	4.32	0.0244

Table 6: (Figure 10)

Calculated coefficients of film heat transfer, based on the unstirred growth rates of the (001) benzophenone face.

$T^{\circ}C$	$\Delta T^{\circ}C$	Growth-rate $cm.sec^{-1}$	Heat produced $cal.sec^{-1}.cm^{-2}$	$h^{*} = \frac{R\ P.\lambda}{\Delta T}$ $cal.sec^{-1}.cm^{-2}.^{\circ}C^{-1}$
39.3	8.7	7.45×10^{-3}	0.1896	0.0218
40.2	7.8	4.00×10^{-3}	0.1018	0.0131
41.0	7.0	2.07×10^{-3}	0.0527	0.00752
42.0	6.0	1.35×10^{-3}	0.0344	0.00573
43.0	5.0	9.71×10^{-4}	0.0247	0.00494
44.0	4.0	6.67×10^{-4}	0.0170	0.00424
44.7	3.3	4.44×10^{-4}	0.0113	0.00342
45.0	3.0	3.05×10^{-4}	0.00776	0.00259
46.2	1.8	1.62×10^{-4}	0.00412	0.00229
46.6	1.4	1.41×10^{-4}	0.00359	0.00256

* Calculated on the basis that growth is entirely heat transfer controlled, and that all the heat is dissipated across the film.

Table 6: cont'd

Calculated coefficients of film heat transfer, based on the stirred growth rates of the (001) benzophenone face.

T°C	$\triangle$ T°C	Growth rate ($cm.sec^{-1}$)	Heat produced ($cal.sec^{-1}cm^{-2}$)	$h^* = \frac{R\rho\lambda}{\triangle T}$ ($cal.sec^{-1}cm^{-2}{}^{\circ}C^{-1}$)
41.1	6.9	6.80×10^{-3}	0.174	0.0251
42.0	6.0	3.42×10^{-3}	0.0870	0.0145
43.0	5.0	2.47×10^{-3}	0.0629	0.0126
44.0	4.0	1.33×10^{-3}	0.0339	0.00846
45.0	3.0	8.78×10^{-4}	0.0224	0.00745
46.2	1.8	4.62×10^{-4}	0.0118	0.00653
47.0	1.0	3.17×10^{-4}	0.0082	0.00807

*Calculated on the basis that growth is entirely heat transfer controlled, and that all the heat is dissipated across the film.

Table 7: (Figure 11)

Experimental coefficients of film heat transfer into unstirred salol melts.

i (amps)	v (volts)	Q ($Cal.sec.^{-1}$)	Thermocouple $\Delta \mu V$	ΔT (^{o}C)	$\frac{Q}{A \Delta T} = h$ ($cal.sec.^{-1}cm^{-2}{}^{o}C^{-1}$)
0.160	1.18	0.047	110	2.59	0.00264
0.200	1.48	0.074	154	3.63	0.00296
0.250	1.83	0.109	210	4.95	0.00336
0.300	2.20	0.157	276	6.50	0.00370
0.350	2.58	0.216	354	8.34	0.00394
0.400	2.93	0.291	434	10.25	0.00416
0.450	3.30	0.368	530	12.50	0.00431
0.500	3.70	0.460	598	14.13	0.00476
0.550	4.05	0.562	686	16.18	0.00502

Table 7: cont'd

Experimental coefficients of film heat transfer into stirred salol melts.

Rate of stirring :- 415 r.p.m.

i (amps)	v (volts)	Q ($Cal.sec^{-1}$)	Thermocouple $\Delta\mu V$	$\Delta T^{o}C$	$\frac{Q}{A\ \Delta T} = h$ $cal.sec.^{-1}cm^{-2}{}^{o}C^{-1}$
0.160	1.18	0.047	66	1.56	0.00438
0.200	1.48	0.074	83	1.96	0.00550
0.250	1.83	0.109	108	2.55	0.00654
0.300	2.20	0.158	124	2.90	0.00829
0.350	2.58	0.216	165	3.89	0.00844
0.400	2.93	0.291	229	5.40	0.00787
0.450	3.30	0.368	277	6.53	0.00824
0.500	3.70	0.460	333	7.88	0.00852
0.550	4.05	0.562	356	8.45	0.00960

Table 7: cont'd

Experimental coefficients of film heat transfer into stirred salol melts.

Rate of stirring :- 810 r.p.m.

i (amps)	v (volts)	Q ($Cal.sec^{-1}$)	Thermocouple $\Delta\mu V$	$\Delta T^{o}C$	$\frac{Q}{A\ \Delta T} = h$ $cal.sec^{-1}cm^{-2}{}^{o}C^{-1}$
0.160	1.13	0.047	32	0.75	0.00910
0.200	1.48	0.074	42	0.99	0.0109
0.250	1.83	0.109	61	1.44	0.0116
0.300	2.20	0.158	80	1.89	0.0127
0.350	2.58	0.216	100	2.36	0.0139
0.400	2.93	0.291	128	3.02	0.0141
0.450	3.30	0.368	169	3.99	0.0135
0.500	3.70	0.460	183	4.32	0.0156
0.550	4.05	0.562	220	5.18	0.0157

Table 8: (Figure 11)

Calculated coefficients of film heat transfer based on the unstirred growth-rates of the (010) salol face.

$T^{\circ}C$	$\triangle T^{\circ}C$	Growth rate ($cm.sec^{-1}$)	Heat produced $cal.sec^{-1}cm^{-2}$	$h^{*} = \frac{R \rho \lambda}{\triangle T}$
40.4	1.6	1.19×10^{-5}	3.25×10^{-4}	2.03×10^{-4}
38.8	3.2	5.85×10^{-5}	1.56×10^{-3}	4.90×10^{-4}
38.3	3.7	8.23×10^{-5}	2.24×10^{-3}	6.13×10^{-4}
38.0	4.0	1.19×10^{-4}	3.24×10^{-3}	8.10×10^{-4}
37.3	4.7	1.42×10^{-4}	3.88×10^{-3}	8.25×10^{-4}
37.1	4.9	1.89×10^{-4}	5.14×10^{-3}	10.5×10^{-4}
36.2	5.8	2.73×10^{-4}	7.44×10^{-3}	12.8×10^{-4}
35.3	6.7	3.44×10^{-4}	9.83×10^{-3}	14.0×10^{-4}
34.2	7.8	4.12×10^{-4}	1.12×10^{-2}	14.4×10^{-4}

*Calculated on the basis that growth is entirely heat transfer controlled, and that all the heat is dissipated across the film.

Table 8: cont'd

Calculated coefficients of film heat transfer, based on the stirred growth rates of the (010) salol face.

T°C	ΔT°C	Growth rate ($cm.sec^{-1}$)	Heat produced ($cal.sec.^{-1}cm^{-2}$)	$h^* = \frac{R.P.\lambda}{\Delta T}$
40.4	1.6	6.69×10^{-5}	1.82×10^{-4}	9.11×10^{-4}
40.0	2.0	1.35×10^{-4}	3.68×10^{-4}	18.3×10^{-4}
39.2	2.8	2.78×10^{-4}	7.58×10^{-4}	27.1×10^{-4}
38.0	4.0	4.76×10^{-4}	1.30×10^{-3}	32.5×10^{-4}
37.6	4.4	5.20×10^{-4}	1.41×10^{-3}	32.2×10^{-4}
37.2	4.8	6.67×10^{-4}	1.81×10^{-3}	37.9×10^{-4}
36.2	5.8	8.35×10^{-4}	2.28×10^{-3}	39.2×10^{-4}
34.5	7.5	1.21×10^{-3}	3.30×10^{-3}	44.0×10^{-4}

*Calculated on the basis that growth is entirely heat transfer controlled, and that all the heat is dissipated across the film.

Table 9: (Figure 12)

Temperature profiles for two crystal-melt interfaces of a salol crystal growing from a melt supercooled 2.5°C in the bulk.

Unstirred growths of the (010) face:-

Distance of interface from thermocouple (cms)	Temperature °C	Distance of interface from thermocouple (cms)	Temperature °C	Distance of interface from thermocouple (cms)	Temperature °C
0.441	39.56	0.199	40.07	- 0.015	40.66
0.425	39.59	0.180	40.12	- 0.060	40.74
0.384	39.59	0.149	40.22	- 0.076	40.78
0.364	39.66	0.119	40.29	- 0.106	40.74
0.307	39.73	0.094	40.34	- 0.130	40.78
0.291	39.76	0.061	40.44	- 0.155	40.76
0.287	39.83	0.042	40.49	- 0.198	40.78
0.230	40.00	0.003	40.59		

Unstirred growths of the (100) face:-

0.54	39.85	0.25	40.34	- 0.04	40.80
0.47	39.91	0.17	40.49	- 0.10	40.80
0.39	40.01	0.10	40.61	- 0.12	40.80
0.32	40.14	0.03	40.73	- 0.20	40.82

cont'd

Table 9: cont'd

Temperature profiles for two crystal-melt interfaces of a salol crystal growing from a melt supercooled 2.5°C in the bulk.

Stirred growths of the (010) face:-

Distance of interface from thermocouple (cms)	Temperature °C	Distance of interface from thermocouple (cms)	Temperature °C	Distance of interface from thermocouple (cms)	Temperature °C
0.115	39.58	0.058	39.58	- 0.015	39.80
0.096	39.58	0.027	39.68	- 0.029	39.92
0.077	39.58	0.000	39.73	- 0.063	39.92

Stirred growths of the (100) face:-

0.326	39.55	0.189	39.58	- 0.000	39.92
0.295	39.55	0.131	39.65	- 0.068	39.92
0.236	39.55	0.071	39.82	- 0.148	39.92

Table 10 (Figures 13, 14, 15, & 16)

The dependence of growth-rates on interfacial temperatures for the (010) face of the salol crystal.

Bulk temperature $T^{o}C$	Interfacial temperature $T_i{}^{o}C$	Bulk supercooling $\Delta T^{o}C$ $(T_m-T)^{o}C$	Interfacial supercooling ΔT_i $(T_m-T_i)^{o}C$	Temperature difference for interfacial film $(T_i-T)^{o}C$	Unstirred growth-rate $cm.sec^{-1} \times 10^{5}$	Stirred growth-rate $cm.sec^{-1} \times 10^{5}$	$\log_{10} R$	$\log_{10}(T_m-T_i)$
35.50	39.05	6.50	2.95	3.45	35.6	-	$\bar{4}.551$	0.470
36.37	39.42	5.63	2.58	3.05	26.0	-	$\bar{4}.415$	0.416
37.10	39.63	4.90	2.37	2.53	23.2	-	$\bar{4}.365$	0.375
37.80	40.04	4.20	1.96	2.24	16.7	-	$\bar{4}.223$	0.292
38.10	39.86	3.90	2.14	1.76	15.7	-	$\bar{4}.196$	0.330
38.50	40.21	3.50	1.79	1.71	12.7	-	$\bar{4}.104$	0.253
38.75	39.37	3.25	2.63	0.62	-	30.0	$\bar{4}.477$	0.420
38.78	40.35	3.22	1.65	1.57	11.3	-	$\bar{4}.053$	0.217
39.15	39.55	2.85	2.45	0.40	-	25.0	$\bar{4}.398$	0.389
39.45	40.14	2.55	1.86	0.69	-	14.1	$\bar{4}.149$	0.269
39.50	40.42	2.50	1.58	0.92	10.3	-	$\bar{4}.013$	0.398
39.35	40.52	2.65	1.48	1.17	9.05	-	$\bar{3}.957$	0.170
39.85	40.61	2.15	1.39	0.76	8.59	-	$\bar{3}.934$	0.143
39.85	40.38	2.15	1.62	0.53	-	8.85	$\bar{3}.947$	0.209
40.00	40.67	2.00	1.33	0.67	6.65	-	$\bar{3}.823$	0.124
40.44	40.73	1.56	1.27	0.29	6.67	-	$\bar{3}.824$	0.104
40.55	40.98	1.45	1.02	0.43	-	3.67	$\bar{3}.563$	0.009
40.75	40.99	1.25	1.01	0.24	3.23	-	$\bar{3}.509$	0.004

Table 11 (Figure 17)

Growth of benzophenone in a capillary of 0.4mm I.D.

M.P. = 48.0°C

Temperature (°C)	Growth-rate $cm.sec^{-1} \times 10^3$	Temperature (°C)	Growth-rate $cm.sec^{-1} \times 10^3$	Temperature (°C)	Growth-rate $cm.sec^{-1} \times 10^3$
45.9	0.0486	38.8	27.7	31.5	83.0
44.8	0.604	37.4	37.8	25.5	96.7
44.6	0.991	36.5	45.8	16.4*	75.8
43.8	2.29	35.6	52.9	16.4	82.0
43.3	4.92	35.1	58.4	14.8*	71.5
42.8	6.24	34.1	65.3	14.8	80.0
42.0	9.82	33.3	69.4		
39.5	22.2	32.5	75.6		

*Capillary I.D. = 0.3mm

Table 12 (Figure 18)

Growth of salol in a capillary of 0.6mm I.D.

M.P. = 42.0°C

Temperature (°C)	Growth-rate $cm.sec^{-1} \times 10^3$	Temperature (°C)	Growth-rate $cm.sec^{-1} \times 10^3$	Temperature (°C)	Growth-rate $cm.sec^{-1} \times 10^3$
39.8	0.03	33.4	1.73	23.9	6.47
39.2	0.06	32.7	2.16	22.4	6.47
38.4	0.13	32.0	2.73	21.8	6.45
37.8	0.15	30.8	3.28	20.7	6.40
37.1	0.20	30.1	3.91	20.2	6.37
36.4	0.25	29.5	4.16	19.3	6.34
35.9	0.75	28.9	4.64	18.5	6.19
35.6	0.42	28.4	5.23	17.0	6.09
35.3	0.87	27.5	5.62	15.5	6.01
34.7	0.53	26.3	6.04	13.5	5.71
34.4	0.34	25.5	6.18	12.4	5.42
34.0	1.32	24.8	6.40	11.1	4.99

Table 13 (Figure 31)

Growth-rate of the (100) face of a salol crystal within a capillary of 1.5mm I.D., at a supercooling of 1.9°C. (Undegassed).

Time (mins)	Growth-rate $cm.sec^{-1} \times 10^5$	Time (mins)	Growth-rate $cm.sec^{-1} \times 10^5$	Time (mins)	Growth-rate $cm.sec^{-1} \times 10^5$
0	13.9	40	9.8	125	7.0
10	12.8	50	9.3	150	6.7
20	11.9	75	8.8	200	5.8
30	10.4	100	7.9	250	4.9

Average growth-rate between t = 270 and t = 1445 mins is $1.43 \times 10^{-5} cm.sec^{-1}$ (Not plotted on graph).

Table 14 (Figure 22)

Growth rate of the (100) face of a salol crystal within a capillary of 1.5mm I.D., from a degassed melt supercooled 3.6°C.

Time (hours)	Displacement (cms)	Time (hours)	Displacement (cms)
2.75	0.070	47.25	1.259
5.41	0.167	49.83	1.342
22.33	0.345	52.25	1.403
28.50	0.484	95.50	1.434

Table 15 (Figure 13)

Growth rate of the (001) face of a benzophenone crystal within a capillary of 0.6mm I.D. at low supercoolings.

Temperature ... 45.4°C ($\triangle T = 2.6°C$)

Time (mins)	Growth-rate $cm.sec^{-1} \times 10^4$
0	9.26
10	3.96
20	2.61
30	1.66
50	1.00
65	0.46
75	1.26
90	0.85
105	0.25

Temperature ... 45.7°C ($\triangle T = 2.3°C$)

Time (mins)	Growth-rate $cm.sec^{-1} \times 10^4$
0	9.78
10	1.81
20	1.12
40	0.42
60	0.93
70	0.60
80	0.15

Temperature ... 46.1°C ($\triangle T = 1.9°C$)

Time (mins)	Growth-rate $cm.sec^{-1} \times 10^4$
0	4.38
10	0.00
20	1.34
30	0.55
60	0.11

Temperature ... 46.3°C ($\triangle T = 1.7°C$)

Time (mins)	Growth-rate $cm.sec^{-1} \times 10^4$
0	1.00
10	0.75
20	0.56
40	0.34
50	0.05

Table 16 (Figure 24)

Removal of impurities by freezing into a solid plug.
Bath temperature ... 37.5°C, capillary I.D. = 1mm, (100) face.

M.P. = 42.0°C

Time (mins)	Growth-rate $cm.sec^{-1} \times 10^6$	Time (mins)	Growth-rate $cm.sec^{-1} \times 10^6$
0	7.55	140	0.28
20	4.76		
40	3.27		
80	1.67		

Table 17 (Figure 25)

Removal of impurities by repeated recrystallisations
(Bath temperature ... 37.5°C, capillary I.D. = 1mm, Salol (100) face).

Run 1		Run 2		Run 3	
Time (mins)	Growth-rate $cm.sec^{-1} \times 10^4$	Time (mins)	Growth-rate $cm.sec^{-1} \times 10^4$	Time (mins)	Growth-rate $cm.sec^{-1} \times 10^4$
0	4.16	0	3.21	0	3.96
10	2.31	10	1.26	10	2.77
20	1.54	20	0.53	20	1.77
30	3.33	30	1.04	25	2.52
40	1.85	40	0.82	30	1.85
62	0.78	60	1.19	40	1.14
90	1.57	80	0.81	60	0.56
120	0.50	110	0.54	100	0.31
140	0.37	130	1.98	140	0.23
180	0.16	150	1.22		
		180	0.72		

Table 18 (Figure 26)

Forced circulation within a capillary of I.D. 1mm.
(Growth of the salol (100) crystal face; immersed in a bath at 38.2°C)

Time (mins)	Growth-rate $cm.sec^{-1} \times 10^4$	Time (mins)	Growth-rate $cm.sec^{-1} \times 10^4$
0	4.90	40	0.74
10	2.31	60	0.40
20	1.40	80	0.26
30	0.97	100	0.17

Table 19 (Figure 47)

The effect of a surface disturbance on the capillary growth rate of benzophenone.

Bath temperature = 46.0°C Supercooling = 2.0°C

Capillary I.D. = 1.5mm (001) crystal face.

Time (mins)	Growth-rate $cm.sec^{-1} \times 10^4$
0	0.02
34	0.01
touched at 34 minutes	
$34\frac{1}{2}$	1.19
40	0.46
45	0.21
50	0.09

Time (mins)	Growth-rate $cm.sec^{-1} \times 10^4$
0	0.00
40	0.00
touched at 40 minutes	
$40\frac{1}{2}$	0.33
70	0.23
75	0.13

Time (mins)	Growth-rate $cm.sec^{-1} \times 10^4$
0	0.87
20	0.64
30	0.45
40	0.35
60	0.24
90	0.09
touched at $90\frac{1}{2}$ minutes	
95	0.48
110	0.41
115	0.20

Table 20 (Figure 28)

The effect of a surface disturbance on the free growth rate of the (010) solid face.

Bath temperature = 40.1°C Supercooling = 1.9 deg C		Bath temperature = 40.4°C Supercooling = 1.6 deg C	
Time	Displacement	Time	Displacement
0	0.000	0	0.000
5	0.020	5	0.015
10	0.038	10	0.028
15	0.054	15	0.044
20	0.068	20	0.059
crystal touched at $20\frac{3}{4}$ minutes		crystal touched at 21 minutes	
25	0.078	25	0.072
30	0.093	30	0.085
35	0.113	35	0.102

APPENDIX II

Physical Data

a) Benzophenone:-

Melting point[a]	48.0°C
Density (solid)[b]	1.083 $g.cm^{-3}$
Latent heat of fusion[b]	23.5 $cal.g^{-1}$

b) Salol:-

Melting point[a]	42.0°C
Density (solid)[b]	1.25 $g.cm^{-3}$
Latent heat of fusion[c]	21.8 $cal.g^{-1}$

c) Copper - constantan thermocouples[d]:-

Temperature	e.m.f. in μV with cold junction in ice
20	787
30	1194
40	1610
50	2035

Ref a: Tamman, 'States of Aggregation'

Ref b: Handbook of Chemistry and Physics (35th Edition)

Ref c: Landolt-Bornstein 'Zahlenwerte und functionen aus Physik Chemie Astronomie Geophysik Technik' II Band, 4 Teil (6 Ausflage)

Ref d: Circular 508, National Bureau of Standards, Washington, D.C.

APPENDIX III.

Nomencleture

A = surface area (cm^2)

B = frequency factor

C_i = a constant for a particular crystal face

f = unspecified function

h = heat transfer coefficient ($cal.sec^{-1}.cm^{-2}.{}^{o}C^{-1}$)

h^* = calculated heat transfer coefficient.

$$\text{Defined as } h^* = \frac{\text{observed rate of growth} \times \rho \lambda}{T_m - T}$$

I = nucleation rate

k = Boltzmann constant

M = molecular weight

m = mass of a molecule

P = vapour pressure

P_{sat} = saturation vapour pressure

ΔP = $P - P_{sat}$

Q = Rate of heat transfer ($cal.sec^{-1}.cm^{-2}$)

R = Gas constant

R_c = condensation rate

R_e = evaporation rate

R_n = net rate of condensation; $R_n = R_c - R_e$

r = particle radius

T = bulk temperature (or absolute temperature cX)

ΔT = bulk supercooling; $\Delta T = T_m - T$

T_m = melting temperature of crystal

T_i = interfacial temperature

ΔT_i = interfacial supercooling; $\Delta T_i = T_m - T_i$

W = work of nucleus formation

α = condensation coefficient

λ = latent heat ($cal.g^{-1}$)

ρ = density ($g.\ cm^{-3}$)

σ = surface tension

APPENDIX IV

References.

1. Volmer, M., Z. Electrochem. 35 (1929) 555
2. Becker, R. von., and Doring, W., Ann Phys., Lpz. 24 (1935) 719
3. Tamman, G., 'States of Aggregation', translated by R.F. Mehl, 1926, London; Constable.
4. Mason, R.E.A., Ph.D. Thesis (University of London) 1963
5. Volmer, M., Z Phys. Chem., 119 (1926) 277
6. Burton, W.K., Cabrera, N., and Frank, F.C., Nature 163 (1949) 398
7. Frank, F.C., Proc. Roy. Soc. (London) A 198 (1949) 205
8. Albon, N., and Dunning, W.J., Acta Cryst., 13 (1960) 495
9. Sears, G.W., J. Chem. Phys. 23 (1955) 1630
10. Bunn C.W., and Emmett, H., Discuss. Faraday Soc., No.5 (1949) 119 - 132
11. Hillig, W.B., 'Cooperstown Symposium' Edited by Doremus, Roberts and Turnbull, 1958, New York; Wiley
12. Butler, R.M., Ph.D. Thesis (University of London) 1950
13. Mason, R.E.A., and Strickland-Constable, R.F., Nature 197 (1963) 897
14. Miers, H.A., 18th Robert Boyle Lecture, Cambridge (1911) 28
15. McCabe, W.L., "Chemical Engineers' Handbook" p 1050 - Edited by Perry, 1950, New York; McGraw-Hill.
16. Ting, H.H., and McCabe, W.L., Ind. Eng. Chem., 26 (1934) 1201
17. Van Hook, A., Ind. Eng. Chem., 36 (1944) 1057
18. Groth, P.H.R. von., 'Chemische Krystallographie' p 102, Vol.5 (1919), Liepzig; Engelmann.

19. Groth, P.H.R. von., 'Chemishe Krystallographie' p 137, Vol.5 (1919), Liepzig; Engelmann.

20. Van Hook, A., 'Crystallisation. Theory and Practice' 1961, New York; Reinhold.

21. Pickardt, E. Von., Zeitschr. f. physik Chemie. 42 (1902) 17

22. Pollatschek, H., Z. Physik Chem. 142 (1929) 289

23. Neumann, K., and Micus, G., Z. Phys. Chem. 2 (1954) 25

24. Hillig, W.B., and Turnbull, D., J. Chem. Phys. 24 (1956) 914

25. Frank, F.C., Discuss. Faraday Soc., No.5 (1949) 48